Response of a Pressurized Water Reactor Dashpot Region to Commercial Drying Cycles

Spent Fuel and Waste Disposition

Prepared for
US Department of Energy
Spent Fuel and Waste Science and Technology

R.J.M. Pulido, A. Taconi, A. Salazar III, R.E. Fasano, R.W. Williams, B. Baigas, and S.G. Durbin

Sandia National Laboratories

April 1, 2022

Milestone No. M2SF-22SN010203032
SAND2022-3813R

DISCLAIMER

This information was prepared as an account of work sponsored by an agency of the U.S. Government. Neither the U.S. Government nor any agency thereof, nor any of their employees, makes any warranty, expressed or implied, or assumes any legal liability or responsibility for the accuracy, completeness, or usefulness, of any information, apparatus, product, or process disclosed, or represents that its use would not infringe privately owned rights. References herein to any specific commercial product, process, or service by trade name, trade mark, manufacturer, or otherwise, does not necessarily constitute or imply its endorsement, recommendation, or favoring by the U.S. Government or any agency thereof. The views and opinions of authors expressed herein do not necessarily state or reflect those of the U.S. Government or any agency thereof.

Prepared by
Sandia National Laboratories
Albuquerque, New Mexico 87185 and Livermore, California 94550

Sandia National Laboratories is a multimission laboratory managed and operated by National Technology and Engineering Solutions of Sandia, LLC, a wholly owned subsidiary of Honeywell International, Inc., for the U.S. Department of Energy's National Nuclear Security Administration under contract DE-NA0003525.

ABSTRACT

The purpose of this report is to document updates to the simulation of commercial vacuum drying procedures at the Nuclear Energy Work Complex at Sandia National Laboratories.

Validation of the extent of water removal in a dry spent nuclear fuel storage system based on drying procedures used at nuclear power plants is needed to close existing technical gaps. Operational conditions leading to incomplete drying may have potential impacts on the fuel, cladding, and other components in the system. A general lack of data suitable for model validation of commercial nuclear canister drying processes necessitates additional, well-designed investigations of drying process efficacy and water retention. Scaled tests that incorporate relevant physics and well-controlled boundary conditions are essential to provide insight and guidance to the simulation of prototypic systems undergoing drying processes.

This report documents testing updates for the Dashpot Drying Apparatus (DDA), an apparatus constructed at a reduced scale with multiple Pressurized Water Reactor (PWR) fuel rod surrogates and a single guide tube dashpot. This apparatus is fashioned from a truncated 5×5 section of a prototypic 17×17 PWR fuel skeleton and includes the lowest segment of a single guide tube, often referred to as the dashpot region. The guide tube in this assembly is open and allows for insertion of a poison rod (neutron absorber) surrogate.

Previously, the apparatus was tested with either an empty guide tube or a poison rod surrogate inserted into the guide tube. This report documents results from testing with an empty guide tube and two fill fluids – deionized (DI) water and 0.2 molar boric acid. Boric acid was tested in the DDA as it is typically added to PWR spent fuel pools (SFPs) as a neutron absorber for criticality control.

A drying procedure was developed for the DDA based on measurements from the process used for the High Burnup Demonstration Project. This test procedure consisted of filling the externally-heated DDA pressure vessel with fluid (either DI water or 0.2 M boric acid), draining the fluid with gravity and multiple helium blowdowns, evacuating additional water with a vacuum drying sequence at successively lower pressures, and backfilling with helium. One test was conducted with water and incorporated improvements to previous DDA testing. Two other tests were conducted with boric acid to simulate SFP conditions more accurately in the DDA and to demonstrate repeatability.

Results indicate that after bulk fluid is removed from the pressure vessel, residual water is verifiably measured through confirmatory measurements of pressure and water content using a mass spectrometer. The final pressure rebound behavior for all three tests was well below the established regulatory limit of less than 0.4 kPa (3 Torr) within 30 minutes of isolation. The two boric acid tests produced very similar temperature and pressure profiles as well as mass spectrometer water content measurements during and after the drying procedure, thus demonstrating repeatability. The water content measurements across all tests showed that despite observing high water content within the DDA vessel at the beginning of the vacuum isolations, the water content drastically drops to below 1,200 ppm_v after the isolations were conducted.

The operational and analytical experiences gained from this test series allow for focus on the dashpot region of the fuel assembly and will guide the transition to full assembly-scale tests at prototypic length. A planned, full-length assembly represents the next evolutionary step in this test series and will feature prototypic assembly hardware, failed fuel rod simulators with engineered cladding defects, and guide tubes with obstructed dashpots to challenge the drying system with multiple retention sites.

This page is intentionally left blank.

ACKNOWLEDGEMENTS

The authors would like to acknowledge the hard work and commitment of all contributors to the project. In particular, we would like to acknowledge the strong support and leadership of Ned Larson at the Department of Energy. Sylvia Saltzstein (SNL) and Geoff Freeze (SNL) are to be commended for their programmatic and technical guidance.

We would like to express our gratitude for the hard work and dedication of our technologists Greg Koenig, Adrian Perales, and Gregory Thad Vice that made the success of this project possible.

This page is intentionally left blank.

CONTENTS

LIST OF FIGURES

LIST OF TABLES

This page is intentionally left blank.

EXECUTIVE SUMMARY

Technical gaps exist in understanding the extent of water removal in a dry spent nuclear fuel storage system with commercial canister drying procedures (Hanson & Alsaed, 2019). Operational conditions leading to substantial amounts of residual water may have potential impacts on the fuel, cladding, and other components in the system, such as fuel degradation and cladding corrosion, embrittlement, and breaching. Additional information is needed on drying process efficacy to evaluate the potential impacts of water retention on long-term dry storage. Given the lack of data suitable for the model validation of drying processes, carefully designed investigations that incorporate relevant physics and well-controlled boundary conditions are needed to supplement existing field data. Experimental components, methodology, and instrumentation are therefore under development for use in advanced studies of realistic drying operations conducted on surrogate spent nuclear fuel.

A small-scale pressure vessel was devised that incorporated a truncated sub-assembly of prototypic pressurized water reactor (PWR) hardware to demonstrate operational capabilities and the utilization of moisture monitoring equipment during drying processes as shown in Figure E-1. The Dashpot Drying Apparatus (DDA) consists of the truncated fuel assembly, a pressure/vacuum vessel, and external heaters to simulate decay heat.

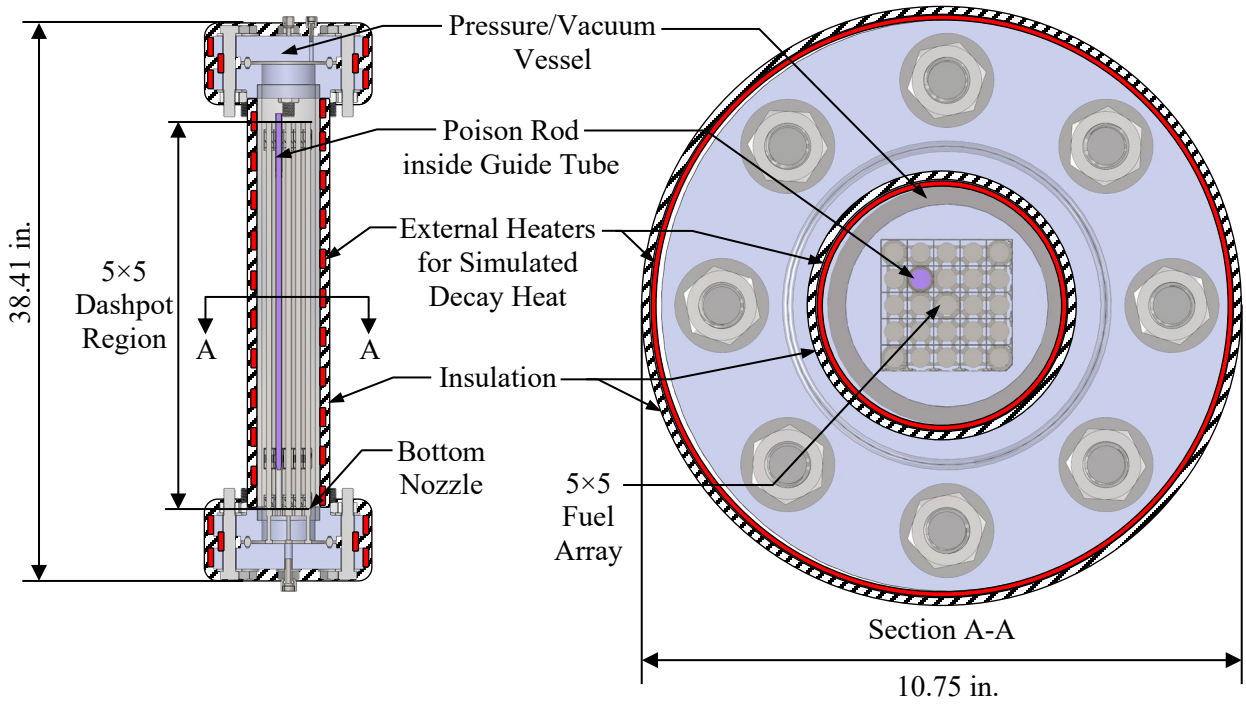

Figure E-1 Major components of the Dashpot Drying Apparatus.

A drying procedure was devised to investigate the efficacy of residual fluid removal after introduction and draining of fluid from the pressure vessel. All tests in this report were conducted with an empty guide tube (no poison rod surrogate was inserted into the guide tube). A mass spectrometer (MS) with specially designed inlets ("HPR-30") was used to monitor moisture and gas composition at various pressure ranges, while other fluid removal behavior was deduced from pressure and temperature measurements.

Two fill fluids were used in the tests documented in this report – deionized (DI) water and 0.2 molar boric acid. Boron, a neutron absorber, is used to control subcritical conditions in spent fuel pools (SFPs) as according to 10 CFR 72.124, Part B, *Methods of criticality control*. The use of boric acid in the DDA was derived from data from reactor SFPs. An International Atomic Energy Agency (IAEA) document from

1982 (IAEA, 1982) as well as a report from Battelle Pacific Northwest Laboratories in 1977 (Johnson, 1977) state that most reactors have SFPs with a concentration of 0.2 M boric acid, corresponding to a roughly 2,200 parts per million by mass (ppm_m) concentration of boron. The IAEA document listed 33 sites that had boron in their SFP, and they varied from 800 ppm_m to 4,000 ppm_m, with most falling between 1,800 ppm_m and 2,200 ppm_m. Therefore, a boron concentration of 2,200 ppm_m was selected. However, as shown from the references, concentrations as high as 4,000 ppm_m and as low as 800 ppm_m would be representative of some SFPs.

A metered amount of fluid (DI water or 0.2 M boric acid) was introduced into the pressure vessel, drained by gravity, and then subjected to multiple blowdowns with helium from 160 kPa to 100 kPa. Afterwards, vacuum drying was performed by implementing sequential isolation points at increasingly lower pressures from 42 kPa (317 Torr) to below 0.013 kPa (0.1 Torr) and monitoring the change in pressure as the system was isolated from the vacuum pump. At the final and lowest pressure, the isolated system pressure was not to exceed 0.4 kPa (3 Torr) after 30 minutes in the final hold in accordance with the regulatory criterion for dryness, as established by NUREG-1536 (NRC, 2010).

Figure E-2 shows the DDA water content in parts per million by volume (ppm_v) measured by a Hiden HPR-30 mass spectrometer, the bottom-most guide tube temperature, and the system pressure during the drying test for a dashpot with an empty guide tube and DI water as the fill fluid. Previously, the power supplied to the external heaters on the DDA was adjusted in real time in an attempt to simulate the temperatures seen in commercial drying. This test implemented a fixed power procedure based on successive iterations of DDA testing. The procedure improved control over testing and allowed thermal behavior to be dominated by the pressure changes in the vessel that arose from either water vapor boiling off the internal surfaces or the introduction of helium backfill.

Figure E-3 shows the DDA water content, the bottom-most guide tube temperature, and the system pressure during the drying test for a dashpot with an empty guide tube and 0.2 M boric acid as the fill fluid conducted on 02/16/22. Another boric acid test was conducted on 03/02/22 and the results were largely identical to the 02/16/22 boric acid test results, thus demonstrating repeatability. These tests implemented the same fixed power procedure as the test using deionized water, so any differences in the thermal behavior of the DDA could be attributed to the change in fluid.

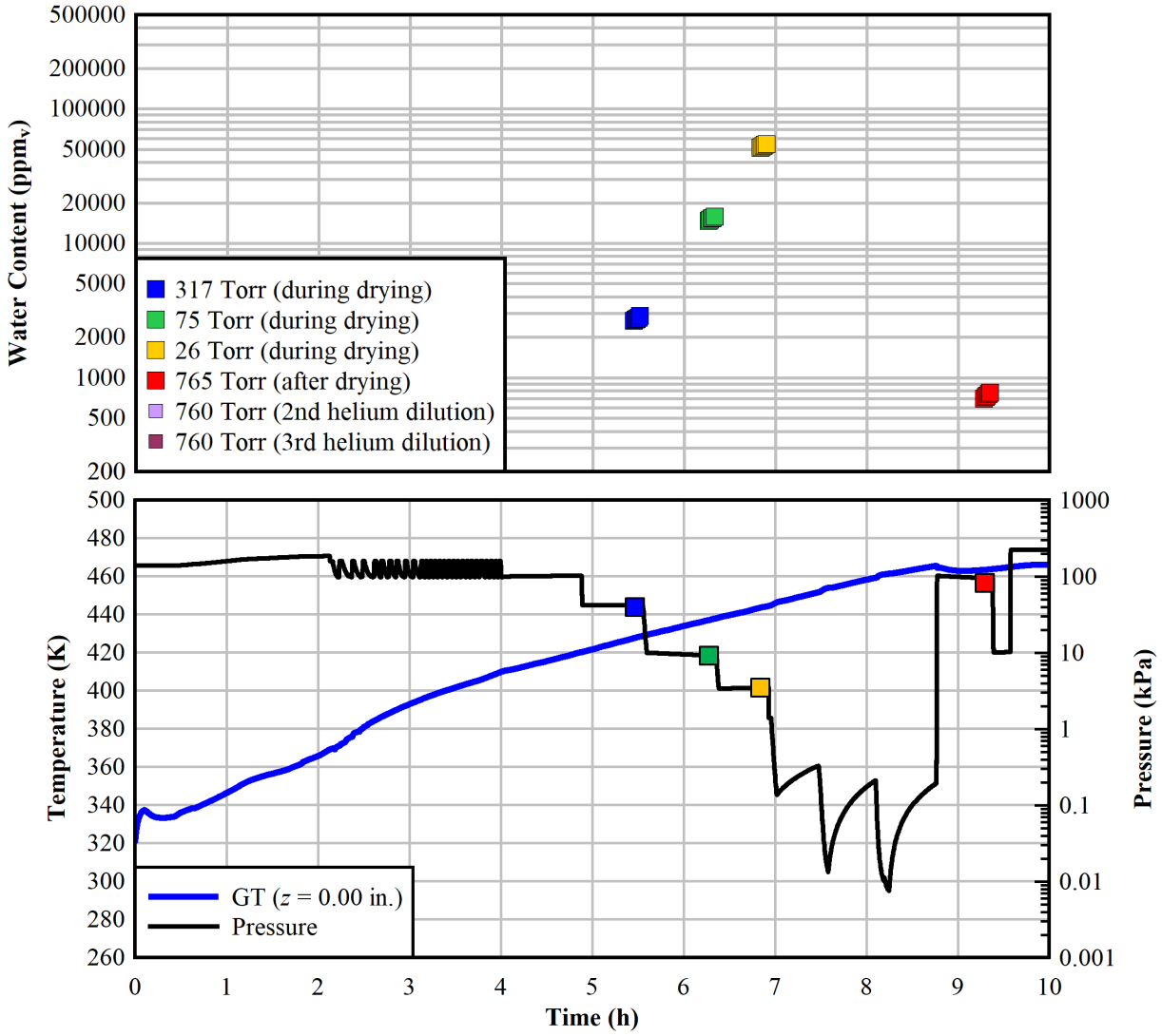

Figure E-2 DDA water content, bottom-most guide tube (GT) temperature, and system pressure during the 02/08/22 drying test using deionized water.

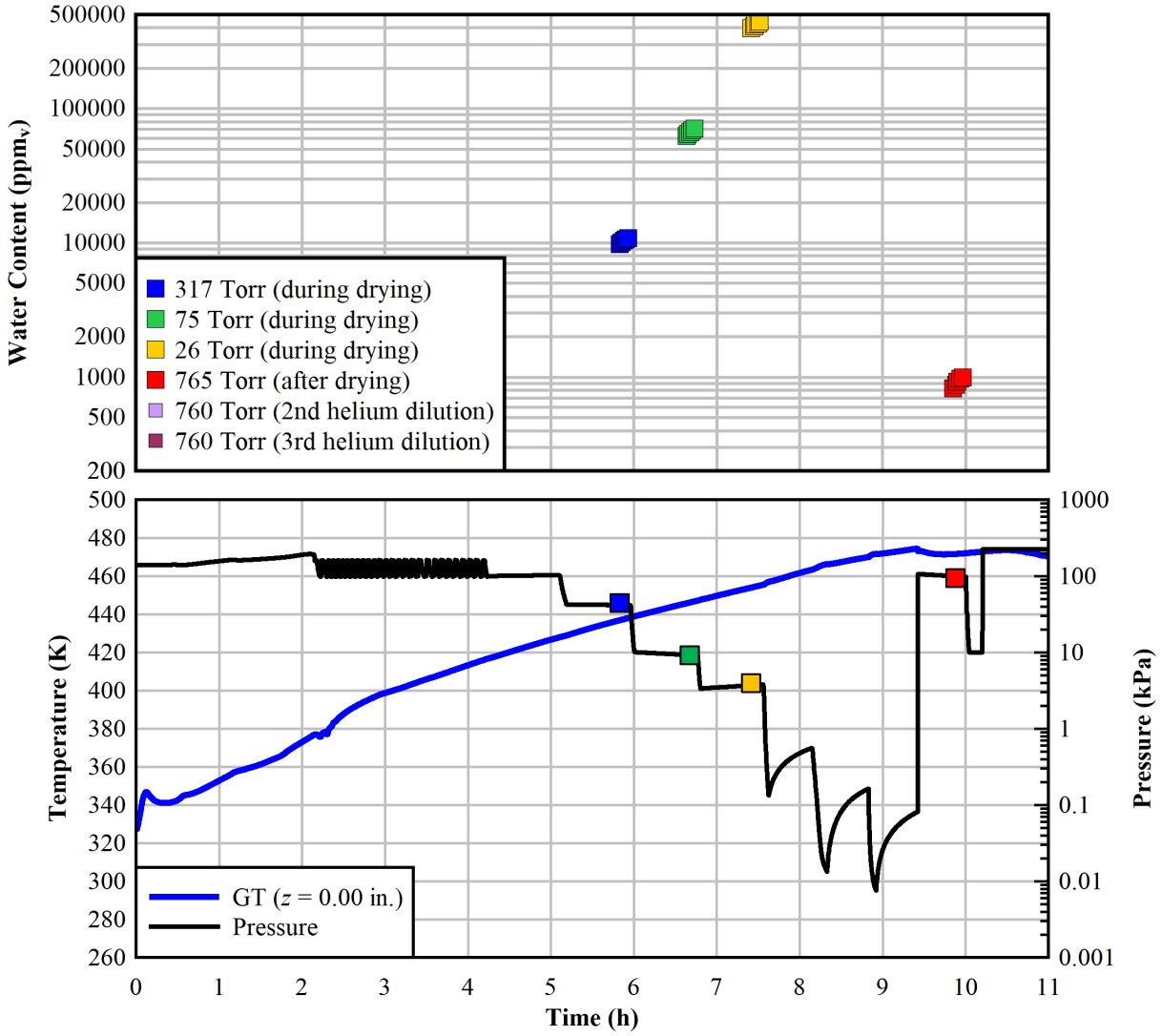

Figure E-3 DDA water content, bottom-most guide tube (GT) temperature, and system pressure during the 02/16/22 drying test using 0.2 M boric acid.

Bulk fluid was observed to be largely removed in post-test mass measurements with loss on the order of ~10 – 20 grams (~0.02 – 0.04 pounds). The measured water content across all three tests showed initially high amounts of water during the drying procedure followed by water content below 1,200 ppm_v following the vacuum isolations. These measurements demonstrated that the DDA was successfully dried following fluid fill to above the surrogate fuel rods.

Results across all DDA tests indicate that temperature histories remained uniform across all tests regardless of fluid type when applying uniform power across each test. Differences in maximum temperatures primarily depended on the test duration, which was influenced by the blowdown period. Pressure histories across all tests showed that all tests met the established regulatory hold criteria of less than 0.4 kPa (3 Torr) in the DDA vessel after an isolation period of 30 minutes.

The two tests with boric acid run on 02/16/22 and 03/02/22 revealed boron concentrations of 2,700 and 2,600 ppm_m, respectively, using inductively coupled plasma optical emission spectrometry (ICP OES). The pH of samples taken pre-fill and post-drain were 4.7 and 4.6 for the 02/16/22 test and 4.8 and 4.8 for the 03/02/22 test, respectively, indicating that the acid concentration in the post-drain samples was

slightly lower. This can be interpreted as some acid remained in the system following the drying procedure. A wash of the DDA was then conducted. These samples had a pH of 5.8, further confirming that some acid remained in the system and was recovered with a wash. The wash samples had a small boron concentration of 50 and 60 ppm_m for the 02/16/22 and 03/02/22 tests, respectively.

The data and operational experience from these tests will guide the next evolution of experiments on a prototypic-length scale with multiple surrogate rods in a full 17×17 PWR assembly. This assembly will feature partially submersible heater rods and a specialized test rod to introduce pre-characterized water retention sites and internal rod pressure monitoring. The insight gained through these investigations is expected to support the technical basis for the continued safe storage of spent nuclear fuel into long term operations.

This page is intentionally left blank.

ACRONYMS / ABBREVIATIONS

DAQ	Data Acquisition
DDA	Dashpot Drying Apparatus
DI	Deionized
DOE	Department of Energy
EPRI	Electric Power Research Institute
FS	Full-Scale
GT	Guide Tube
HBDP	High Burnup Demonstration Project
IAEA	International Atomic Energy Agency
ICP OES	Inductively Coupled Plasma Optical Emission Spectrometry
ISFSI	Independent Spent Fuel Storage Installation
MS	Mass Spectrometer
NIST	National Institute of Standards and Technology
ppm_v	Parts Per Million by Volume
ppm_m	Parts Per Million by Mass
PV	Pressure Vessel
PWR	Pressurized Water Reactor
RSD	Relative Standard Deviation
RTJ	Ring-Type Joint
SCR	Silicon-Controlled Rectifier
SFP	Spent Fuel Pool
SFWST	Spent Fuel and Waste Science and Technology
SNF	Spent Nuclear Fuel
SNL	Sandia National Laboratories
TC	Thermocouple
VCR	Vacuum Coupling Radiation
WVIA	Water Vapor Isotope Analyzer

This page is intentionally left blank.

RESPONSE OF A PRESSURIZED WATER REACTOR DASHPOT REGION TO COMMERCIAL DRYING CYCLES

This report fulfills milestone report M2SF-22SN010203032 in the Spent Fuel and Waste Science and Technology (SFWST) work package (SF-22SN01020303). This work was sponsored under the Department of Energy's (DOE) Office of Nuclear Energy (NE) Spent Fuel and Waste Disposition campaign.

1 INTRODUCTION

1.1 Objective

Numerous water retention sites may exist within the internal volume of a multi-assembly dry storage system that require a specialized approach for the evacuation of water. While guidelines exist on ensuring sufficient evacuation of water from assembly cavities, there is a lack of time-dependent data on water removal from full-scale commercial drying procedures. Obtaining such data has been identified as a high-priority research topic to advance the technical basis for the long-term management of spent nuclear fuel (SNF) (Hanson & Alsaed, 2019). Operational conditions leading to incomplete drying may have potential impacts on the fuel, cladding, and other components in the system.

Drying procedures have been simulated in the laboratory (Colburn, 2021; Knight, 2019) and data has been obtained from samples of canisters subjected to commercial drying processes (Bryan *et al.*, 2019). While transient vacuum drying data has been analyzed for a small-scale apparatus in previous studies at Sandia National Laboratories (SNL) (Salazar *et al.*, 2020), additional information is needed to evaluate the potential impacts of water retention on extended long-term dry storage for a commercial cask system. This includes unique locations in prototypic fuel assembly and canister hardware where water may be more difficult to remove, such as dashpots. Direct measurement of residual water in scaled systems representative of commercial systems is therefore necessary to advance the current technical understanding of the drying procedures used by industry.

This report documents tests conducted on a truncated pressurized water reactor (PWR) sub-assembly that incorporates several important prototypic geometries that will be present in the full-length assembly tests to be conducted in the near future. This chapter will discuss the motivating issues underlying the investigation and a summary of past tests that were designed to respond to some of these concerns. Chapter 2 will discuss development of the instrumentation, equipment, and procedures for the test series, including moisture-monitoring equipment. Chapter 3 will discuss the results of the tests, while Chapter 4 will summarize the findings of the investigation and discuss future work.

1.2 Prototypic Thermal-Hydraulics

Prototypic hardware is incorporated to mimic the important geometries found in dry storage systems. One goal of this testing is to preserve actual fuel assembly geometry and associated retention sites for residual water.

Figure 1-1 shows locations within a PWR fuel assembly that can serve as water retention sites, such as the mixing vanes and bulge joints of the grid spacers. The fuel assembly features guide thimble tubes for the insertion of control rods or burnable poison assemblies which function as neutron absorbers for criticality control in the reactor. The dashpots in the guide tubes are designed to drain water through a centrally located through-hole in the guide thimble bolt (i.e., vent hole). If the vent hole is fouled during reactor operations or pool storage, the dashpot could conceivably retain bulk water during the initial draining operations preceding canister drying. However, the water would be free to communicate with the interior of the canister via the flow holes and the open top of the guide thimble during drying operations.

Burnable poison rods are inserted and left in some fuel assemblies, which could restrict the flow area for any trapped water in the dashpot region if the vent hole is fouled.

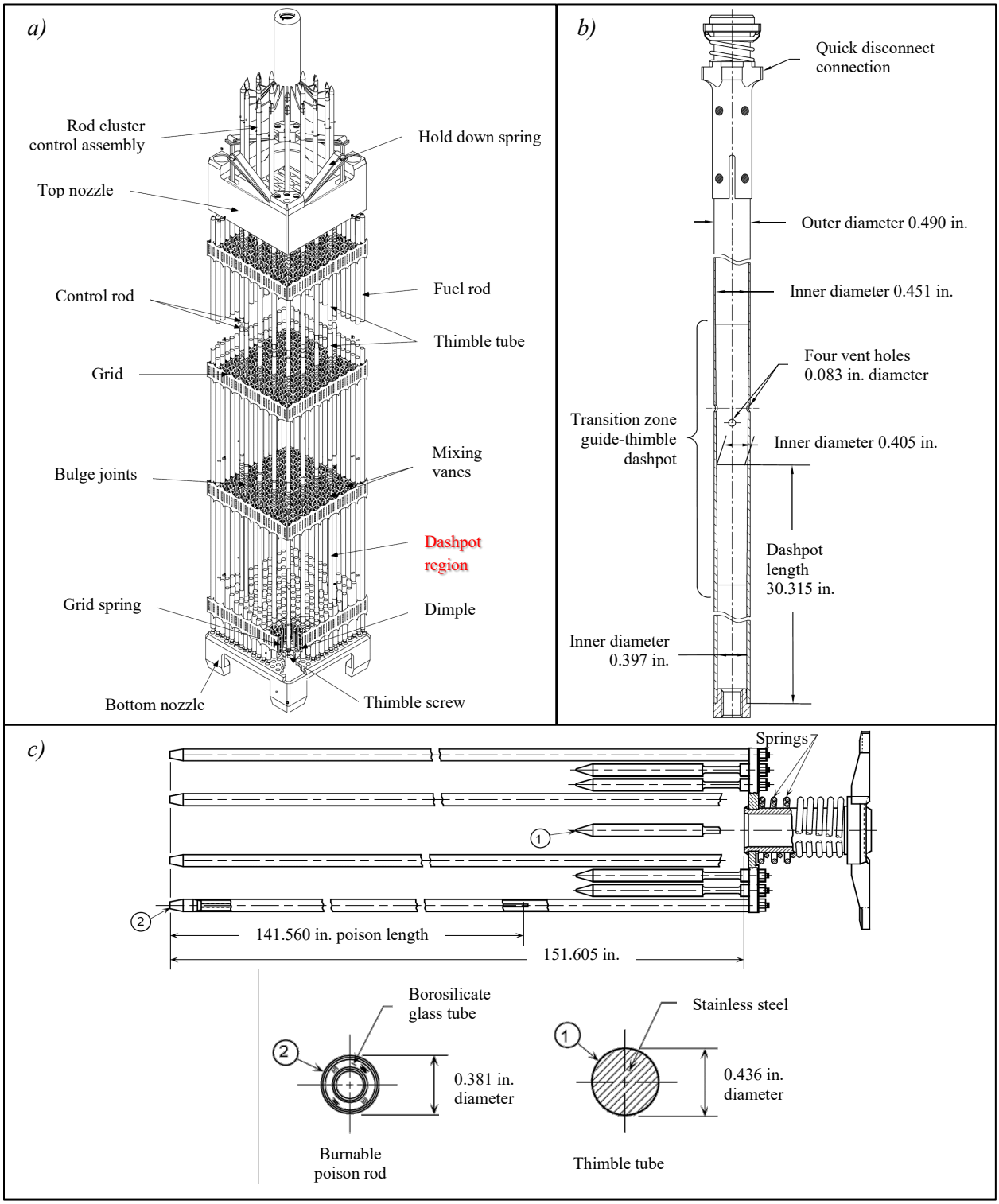

Figure 1-1 Water retention sites exhibited in *a)* a typical 17×17 PWR fuel assembly construction, *b)* a typical PWR guide thimble tube, and *c)* a burnable poison rod assembly (Figures 3.1-16, 4.2-8, and 3.1-26 in NRC, 2002a).

1.3 Residual Water

Spent fuel assemblies are dried after interim storage in pools to ensure the removal of water in assembly cavities as a defense against issues related to pressurization and corrosion that might occur during the subsequent dry storage process, which may extend into the long term. The evacuation of most water and oxidizing agents contained within the canister is recommended by NUREG-1536 (NRC, 2010). A pressure of 0.4 kPa (3 Torr) is recommended to be held in the canister for at least 30 minutes while isolated from active vacuum pumping as a measure of sufficient dryness in the canister. A similar drying method developed at Pacific Northwest National Laboratory (PNNL) is suggested (Knoll & Gilbert, 1987), where less than 0.25 volume percent (2,500 parts per million by volume, or ppm_v) of oxidizing gases are left in the canister (1 mole in 7 m^3 at 150 kPa and 300 K).

An industry standard guide was established for the drying of SNF after cooling in spent fuel pools (SFPs) (ASTM, 2016). The main purpose of the standard is to aid in the selection of a drying system and a means of ensuring that adequate dryness is attained. Examples of typical commercial processes are documented in the standard, where there is adherence to the aforementioned 0.4 kPa (3 Torr) level when discussing the measurement of pressure rebounds. However, there are no substantial details on the utilization of moisture content measurements to ensure adequate water removal, and the establishment of related dryness metrics are deferred to regulatory agencies. There is only a broad recommendation to impose drying conditions that maximize moisture removal from the system.

Water remaining in canisters upon completion of vacuum drying can lead to corrosion of cladding and fuel, embrittlement, and breaching. There is also some risk of creating a flammable environment from free hydrogen and oxygen generated via the radiolysis of water. The remnant water may be chemically absorbed (chemisorbed), physically absorbed (physisorbed), frozen, or otherwise trapped in cavities, blocked vents, breached clads, damaged fuel, etc. Chemisorbed water is bound to components by forces equivalent to a chemical bond, such as the formation of hydroxides and hydrates on zirconium, or corrosion products on the fuel or cladding. Physisorbed water is bound to components by weaker forces (e.g., Van der Waals, capillary) as an adsorbate, and increased surface area provided by material defects enhances this effect. Boric acid has also been known to corrode carbon steel and low alloy steel (NRC, 2011).

The removal of unbound water is largely dependent on the geometry and tortuosity of the components and the speed of the drying process. Cladding breaches are notable cases in that water can become trapped inside a fuel rod between fuel pellets and absorbed in cracks and voids. Water vapor may continue to be diffusively released after the application of vacuum has ended. Depending on the thermal profile, condensation may occur on the cooler surfaces of the canister and internal hardware, such as those lying at the lower extremes distant from heat-emitting SNF.

The pressure applied during vacuum drying lies below the water vapor pressure. Given the unique heat retention and phase change properties of water, when significant heat is removed during volatilization, some quantity of liquid may freeze (ASTM, 2016), thereby inhibiting water removal. It is therefore important to understand under what marginal conditions ice may form during the procedure. Careful control of the vacuum pumps may prevent ice formation by controlling suction near pressures liable to introduce liquid-to-solid phase transitions. Further mitigation may be achieved by implementing pressure reduction in stages that involve bringing the temperature to equilibrium with hot inert gases like helium prior to commencement of the next stage. In a general expansion of this concept, further research and development on forced helium dehydration (FHD) has been recommended to address recently identified technological gaps (Hanson & Alsaed, 2019).

If vacuum is employed to remove water from a canister, measurements in the pressure response to intermittent pump operation may serve as a good indicator of residual, unbound water (ASTM, 2016). Such an approach would involve analysis of the time-dependent pressure rebound when the vacuum pump is isolated from the system. The system is considered adequately dry if the system pressure remains below

0.4 kPa (3 Torr) for at least 30 minutes. Monitoring the moisture content in gas removed from the canister is also suggested as a means of evaluating adequate dryness. Dew point monitoring and spectroscopic techniques could be used to this end, although these measurements must be benchmarked to understand how they scale to various levels of dryness.

1.4 High Burnup Demonstration

The High Burnup Demonstration Project (HBDP) spent fuel data project from the DOE SFWST program is an ongoing research platform to examine the performance of high burnup spent nuclear fuel in dry storage systems. The project included the loading, drying, and storage of an Orano TN-32B at the Independent Spent Fuel Storage Installation (ISFSI) at the North Anna Nuclear Power Station in Virginia.

1.4.1 Transient Vacuum Drying Data

Data are available on the drying procedures employed in the transfer of the assemblies to the decontamination bay and subsequent loading into the TN-32B (EPRI, 2019) along with STAR-CCM+ and COBRA-SFS model validation (Fort *et al*., 2019). These data include ambient temperatures at the facilities, cask surface temperatures, and fuel temperatures, along with additional measurements for long-term cask monitoring. Of particular importance to this report are the data obtained and analyzed for the transients observed during the loading and vacuum drying processes. That is, time-dependent measurements from the HBDP are poised to inform the test setup for this scaled demonstration with prototypic hardware.

The SNF within the TN-32B was put through a prototypic loading and drying process with some minor exceptions involving the installation of instrumentation. The process proceeded as follows:

1. Loading of SNF assemblies from the spent fuel pool into the submerged cask.
2. Movement of the cask into the decontamination bay and installation of the draining and drying equipment.
3. Drainage of the cask using helium as a cover gas.
4. Multiple blowdowns of the cask until bulk flow of liquid water was visually observed to cease.
5. Vacuum drying of the cask using successive stages of increasingly low pressures until the pressure was observed to not exceed 3 Torr within 30 minutes when the cask was isolated.
6. Backfilling of the canister with helium to 222 kPa (1665 Torr).

For the scaled test, the simulation capability of the experimental apparatus can accommodate water filling (representing the cask loading within the pool and the transfer period), drainage, blowdown, vacuum drying, and backfilling. Table 1-1 shows the elapsed times for major events during the HBDP drying processes starting with the beginning of the water draining. This sequence of events, and the resulting temperatures and pressures in the fuel and cask, sets the values for which the DDA tests were conducted to replicate.

The peak measured temperature during vacuum drying was 237 °C, which occurred at the center of the cask slightly above the mid-plane eight hours after the start of vacuum drying (EPRI, 2019). Due to the offset of the thermocouple lance, this maximum implied a peak cladding temperature of 240 °C, which is well below the regulatory limit of 400 °C. The maximum steady-state measurement of 231 °C was obtained during the helium backfill. The maximum external cask surface temperature was 88.3 °C near the cask midplane as measured 12 days after the backfill with helium.

Table 1-1 Elapsed times for the TN-32B water removal and backfill procedures from the HBDP (EPRI, 2019).

Procedure	Elapsed Time (h)
Begin drain	0.00
Finish drain	0.72
Begin blowdowns	4.63
Finish blowdowns	7.18
Begin vacuum drying	7.22
Vacuum drying complete	14.31
Begin initial helium backfill	15.63
Begin final helium backfill	16.22
Finish backfill	17.03

1.4.2 Gas Sampling for High Burnup Demonstration Project

Prior to transportation to the ISFSI, samples of the helium backfill gas were collected at 5 hours, 5 days, and 12 days after the drying process (Bryan *et al.*, 2019). Samples were obtained in 1 L cylinders pressurized to 20 psig. Gas samples were analyzed first at room temperature by Dominion Energy using a gas chromatograph. They were then re-analyzed in a more thorough manner with heating at SNL to mitigate sorption effects in the sample bottles. Mass spectrometry was used to quantify bulk and trace gases in the sample while a humidity sensor was used to measure water content.

The Dominion water content analysis employed a Los Gatos Research Water Vapor Isotope Analyzer (WVIA). The instrument is designed for ambient vapor analysis in the field using an absorption technique with an optical cavity measurement cell. Although it operates best with a continuous flow stream, the North Anna cask could not be sampled directly as a failure scenario would result in a release pathway to the decontamination bay. Therefore, the static samples were employed instead and analyzed continuously while connected to the WVIA. The measured water content was 1,633, 8,896, and 8,300 ppm_v for samples 1-3, respectively.

The MS employed in the SNL analysis was a Finnigan MAT 271 high-resolution MS specialized for hydrogen isotope measurements via a stable gas ionization source. The instrument employs a combination Faraday cup and secondary electron multiplier for measurement of bulk and trace gases, respectively, and it was calibrated using a precision gas mixture. Measurements were obtained with a 50 cm^3 sample cylinder in line with a high vacuum system using an established high-purity sample and measurement procedure. Water was able to be measured, but its content was underestimated when present as a trace gas and overestimated when present in higher concentrations due to the adsorption-desorption effects that occur during sample introduction into the cylinders as well as during the sample transfer within the stainless steel high vacuum system. Therefore, only estimates of the water content could be provided by the MS due to sorption effects in the sample chamber. However, valuable insight was gained on radiolysis and the formation of anoxic corrosion byproducts and hydrogen gas. Also, no fission gases were detected in the analyses, indicating a lack of fuel failure during cask loading.

The ultimate sensor used for water content measurement at SNL was a Vaisala model HMP77B relative humidity probe mounted to the sample bottle on a tee with a pressure gauge. With an operating range of -70 °C to 180 °C, the probe could be placed directly in an oven during sample heating. It was also capable of static measurements but valves in the vacuum line required some period of time for the system to re-settle for a given adjustment. Measurements were obtained at temperatures ramping up to 65 °C. Water content was found to be 10,000 $ppm_v \pm 1{,}000$ ppm_v and 17,400 $ppm_v \pm 1{,}740$ ppm_v five and twelve days after drying, respectively, ultimately indicating that 100 grams of water remained in the gas phase in the cask. (The measurements of the 5-hour sample were affected by a leak, but the room temperature measurement was 2,097 ppm_v). However, because the relative humidity was less than the anticipated 10%

at 85 °C at the time of sampling, no liquid water was found to exist within the canister unless trapped in locations inaccessible to the drying system.

Given the method of sampling from the HBDP, it may not be possible to implement an MS or humidity probe in a canister with live SNF. Regulatory guidelines present limitations in the type of data that can be obtained in a commercial system. For example, it may not be possible to sample gas for mass spectrometry from the vacuum drying process using a slip stream.

1.4.3 Scaled Demonstration

Figure 1-2 shows a conceptual vertical cross-sections through the HBDP cask and the DDA. Figure 1-2a on the left is adapted from Figure 1.2-1 in TN-32 Final Safety Analysis Report (FSAR), Revision 2 (NRC, 2002b). Figure 1-2b on the right shows the DDA. The DDA is designed to represent one dashpot from a single fuel assembly surrounded by a 5×5 fuel array and will be described in detail in Chapter 2. This representation introduces scaling distortions between the DDA and the HBDP cask, which contains multiple full-length assemblies, a basket surrounding the assemblies, and neutron poisons. These additional components in the HBDP cask compared to the DDA serve to increase the number of potential water retention sites through a larger surface area ratio of canister internals to canister wall (40:1 for the HBDP cask assuming all assemblies are 14×14 versus 2.5:1 for the DDA). It is acknowledged that the interpretation of the measured water content in the DDA during and following the simulated drying procedure will thus be affected by these scaling distortions.

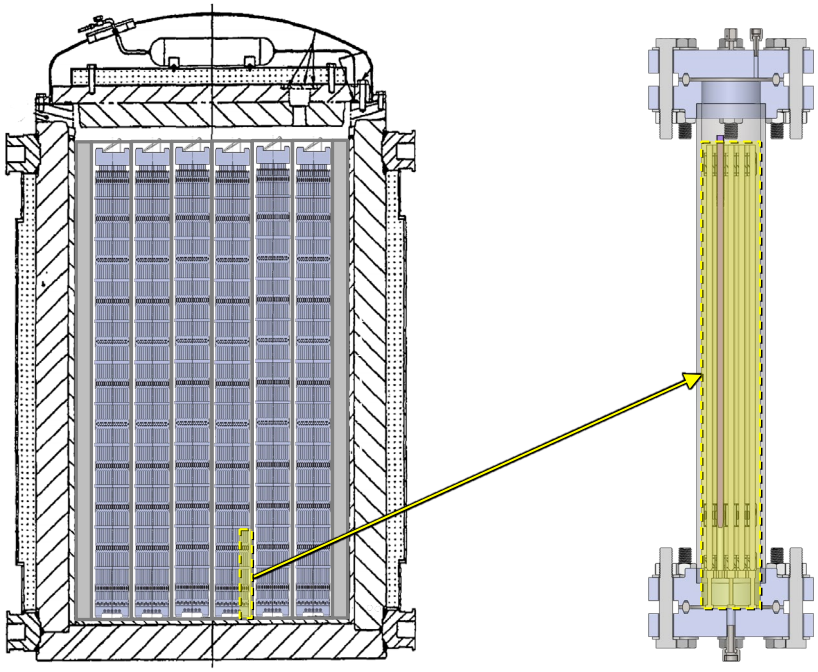

Figure 1-2 Cross-sections showing a) portion of fuel from the High Burnup Demonstration Test represented by b) the Dashpot Drying Apparatus.

2 DEVELOPMENT AND TESTING

This chapter will discuss the testing setup and methodology that aims to address gaps in the current understanding of vacuum drying and residual water analysis that were previously covered in SAND2021-11828 R, "Update on the Simulation of Commercial Drying of Spent Nuclear Fuel," (Durbin *et al.*, 2021), SAND2020-5341 R, "Development of Mockups and Instrumentation for Spent Fuel Drying Tests," (Salazar *et al.*, 2020), and SAND2019-11281 R, "Advanced Concepts for Dry Storage Cask Thermal-Hydraulic Testing" (Salazar *et al.*, 2019).

2.1 Test Objectives

Tests were conducted to verify the removal of residual water in a stainless-steel pressure vessel (4.5 inch OD, 3.826 inch ID) with an integrated prototypic dashpot as a potential water retention site in the DDA system. This system allows for thermal-hydraulic investigations of drying efficiency with prototypic hardware.

The main objectives of the tests include the following:

1. Demonstrate that a drying procedure can be implemented to remove water retained in the pressure vessel, where pressure measurements can confirm minimal rebound pressures after the application of several vacuum isolation points
2. Refine procedures and provide diagnostics for system equipment and moisture monitoring instrumentation, in particular the use of mass spectrometry

Performance verification in this test series with the DDA will support more advanced drying tests employing heater rods and specialized rods in a full-size assembly. In turn, data can be provided that are readily scalable to commercial dry cask storage and transportation applications.

2.2 Fuel Assembly and Fill Fluid

2.2.1 Fuel Assembly Details

The PWR sub-assembly was harvested by cutting out a 5×5 section from one corner of a 17×17 PWR skeleton, which included one guide tube dashpot attached to the lowest grid spacer and the debris catcher. The concept is shown in Figure 2-1, and a photo of the assembly is shown in Figure 2-2.

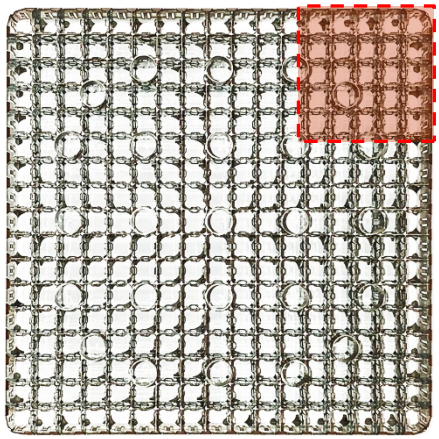

Figure 2-1 Concept for taking 5×5 subassemblies from a 17×17 PWR skeleton. The sub-assembly placed in the pressure vessel was taken from one of the corners (red).

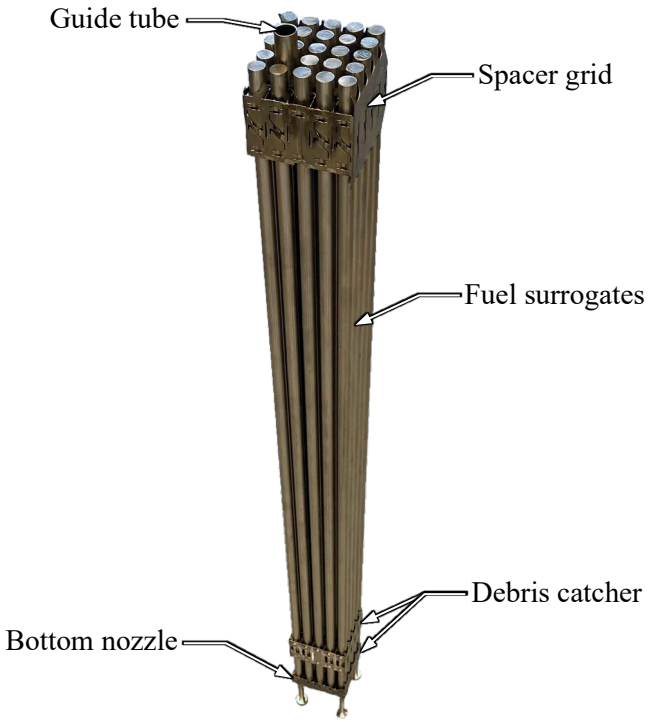

Figure 2-2 Photo of the 5×5 sub-assembly. The guide tube was left empty for all tests.

The rod layout for the sub-assembly is shown in Figure 2-3. Fuel rod surrogates were placed in the locations in the assembly labeled in red. All tests documented in this report were conducted with an empty guide tube – no poison rod surrogate was inserted into the guide tube.

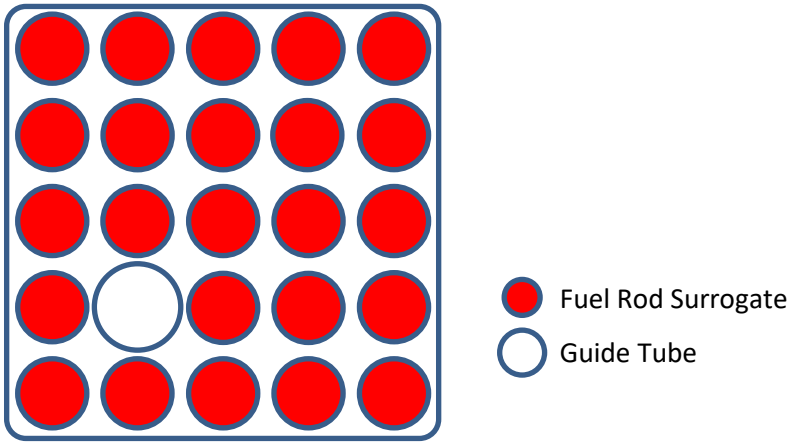

Figure 2-3 Rod layout for a 5×5 mini assembly.

2.2.2 Fill Fluids

The vacuum drying procedure was tested three times, with the two types of tests documented in this report distinguished by the fluid used during the filling step. Deionized (DI) water was used to develop a baseline test to compare the thermal profiles across the DDA throughout the drying procedure to those seen during two tests using 0.2 M boric acid as the fill fluid.

The use of boric acid in the DDA was inspired by data from reactor SFPs. Boron, a neutron absorber, is used as a criticality prevention measure in accordance with 10 CFR 72.124, Part B, *Methods of criticality*

control. An IAEA document from 1982, as well as a report from Battelle Pacific Northwest Laboratories in 1977 (Johnson, 1977), mention that most reactors have SFPs with a concentration of 0.2 molar boric acid, corresponding to roughly 2,200 parts per million by mass (ppm_m) concentration of boron. The IAEA document listed 33 sites that had boron in their SFP, and they varied from 800 ppm_m to 4,000 ppm_m, with most falling between 1,800 ppm_m and 2,200 ppm_m. In a report to the NRC in 2001, the Palisades Nuclear Plant mentions having their SFP at 3,000 ppm_m (Harden, 2001). The Comanche Peak Steam Electric Station stated their SFP has a concentration around 1,900 ppm_m (Comanche Peak Steam Electric Station, 2000). San Onofre's boric acid backup tanks have a concentration of 11,000 ppm_m for boric acid, which corresponds to a boron concentration of about 1,800 ppm_m (Combustion Engineering, Inc., 1986). Therefore, a boron concentration between 1,800 and 2,200 ppm_m was selected. However, as shown from the references, concentrations as high as 4,000 ppm_m and as low as 800 ppm_m would be representative of some SFPs.

2.3 Pressure Vessel and Test Setup

A pressure vessel (PV) was constructed of nominal four-inch 316 stainless-steel schedule 80 pipe terminated with welded flanges. The flanges are connected to blinds by ring-type joints (RTJs). Penetrations into the PV are made via welded glands with vacuum coupling radiation (VCR) face seal connections. A photo of the pressure vessel is shown in Figure 2-4, and a photo of the complete test setup is shown in Figure 2-5.

All VCR connections are sealed with unplated, non-retaining stainless-steel gaskets. Leak testing was conducted using the leak test ports on the female VCR nuts and measuring increases in pressure in the evacuated system. The MS was also employed to test for leaks using helium – a background helium concentration was established first, and then subsequent MS measurements were analyzed for spikes when flowing helium in the direction of a given port.

The top and bottom flanges are sealed with stainless-steel octagonal ring-type gaskets. In preliminary testing with a small vessel using these flanges, these gaskets were observed to have a relatively minimal dry leak rate compared to other options (i.e., carbon steel and/or oval ring). The leak rate was evaluated as 2.3×10^{-5} cm^3/s according to the ANSI-N14.5 specification for radioactive material transport packages after correcting from pressurized helium to air and leakage from 100 kPa to 1 kPa. However, measurements were found to be impacted by leakage in the plumbing lines, so results could only be used on a comparative basis.

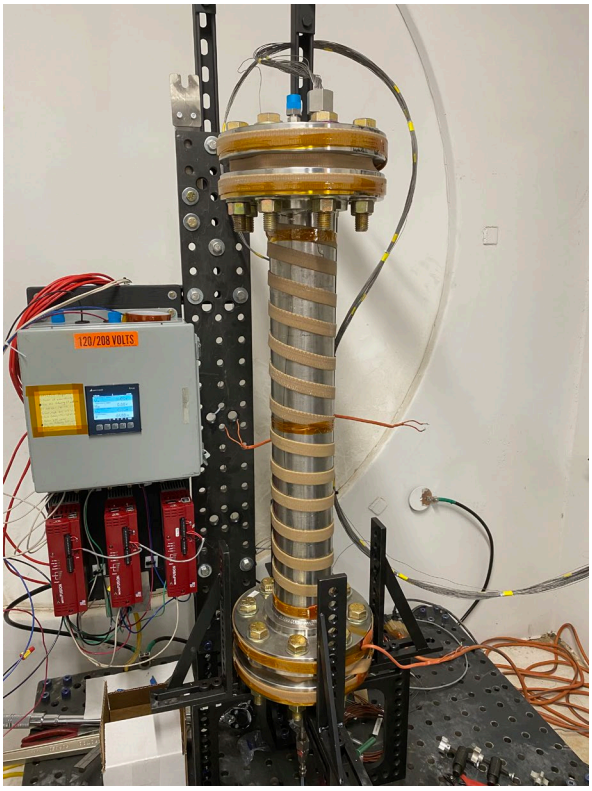

Figure 2-4 Photo of the pressure vessel used for the 5×5 DDA testing. Flexible heaters were wrapped around the pressure vessel to provide simulated decay heat.

Figure 2-5 Photo of the complete DDA drying test setup.

A diagram of the test setup including the pressure vessel is shown in Figure 2-6. Bellows-sealed valves form the boundaries to the main internal volume of the PV. The left PV isolation valve leads to the main

vacuum pump line (green), consisting of a Leybold EcoDry 40+ scroll pump and a Leybold MAG W 300 iP turbo pump, as well as the MS (purple), which uses an Edwards nXDS6i scroll pump and an Edwards nEXT070 turbomolecular pump to maintain a high vacuum within its sample chamber. For testing with boric acid, a vacuum filter was added to protect the vacuum pump. To dry out the MS and ensure that water content measured during sampling was solely derived from the fill fluid, a drying gas line (orange) was supplied with both nitrogen and helium to perform bulk drying with nitrogen followed by establishment of a helium background in the MS. A Setra 100 Torr transducer was added to the vacuum line to ensure consistency in pressure measurements between the vacuum and pressure lines when both were exposed to the pressure vessel at 100 Torr or below. The right PV isolation valve leads to the branch with MKS and Setra pressure transducers as well as the helium pressurization line (red), while the bottom flange isolation valve is used for water filling and draining (blue).

Altogether, the vacuum-tight design minimizes leakage and allows for fine control of both sub-atmospheric pressures and high pressures up to 1,000 kPa. The pressure vessel has been designed to minimize separation between assembly components and instrumentation through the use of blind flanges with penetrations for thermocouples (TCs) and instrumentation. Thermocouples are fed through a Viton packing in a compression fitting on the upper flange. This method of installation was permanent and prevented the replacement of gaskets or faulty TCs.

The pressure vessel was mounted on a stand comprised of fixture table components and steel framing. This stand also supported peripheral plumbing lines and provided a convenient location for the MS sample block to minimize the length of the sample line tubing.

Improvements based on lessons learned from previous DDA testing (Durbin *et al.*, 2021) were implemented for the tests documented in this report. Heat trace cabling was added to the helium pressurization, vacuum pump, and MS lines to eliminate cold spots in those areas and prevent water condensation, which could skew interpretations of water content in the PV. Prior to each test documented in this report, the DDA and the external lines were dried by applying heat to the pressure vessel and applying vacuum, removing any residual water from condensation of atmospheric moisture and previous tests. The MS was then used to sample from the system to measure the level of dryness in the PV – the DDA was considered ready for testing when the water content in the system dropped below 100 ppm_v. With these considerations, the potential for fluid to condense is greatly reduced, allowing the sampled gas to remain representative of the PV contents.

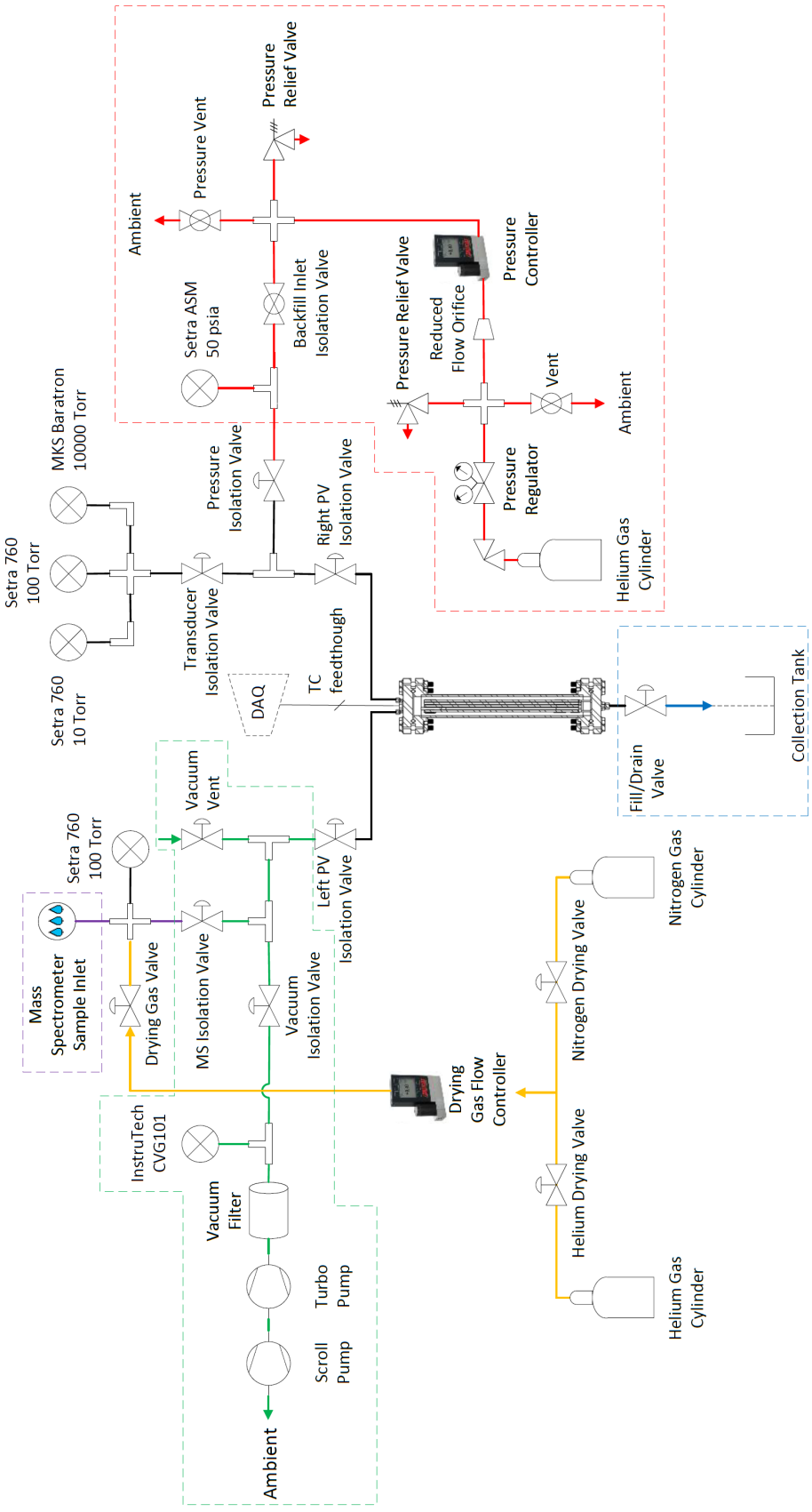

Figure 2-6 Diagram of DDA pressure/vacuum system.

In addition, an iterative testing procedure was conducted to establish uniform power supply to the heaters during testing. Controlling the power supply as a function of time consistently across tests allowed for improved clarity in the attribution of differences in thermal behavior among the datasets, as the procedure eliminated power supply as an independent variable.

2.4 Bulk Fluid Filling and Draining

The pressure vessel is filled with fluid (either deionized (DI) water or 0.2 M boric acid) through a flexible hose connected to the bottom valve in the lower blind flange as shown in Figure 2-6. The system can be drained via the same plumbing by opening the fill/drain valve with further draining aided by pressurized blowdowns.

To determine the internal volume of the pressure vessel, a container of DI water was weighed using a Mettler Toledo PBD655 bench platform (repeatability 1.3 g), and the water in the container was then poured into the vessel. The DI water container was weighed following pours at two different fill levels – the first level was taken at the top of the fuel rod surrogates, while the second level was taken at the top of one of the VCR fittings on the top flange to determine the maximum volume of the pressure vessel. The container weights before and after the pour as well as the corresponding vessel water contents by weight at the two fill levels are listed in Table 2-1.

Table 2-1 Pressure vessel water volumes by weight at two different fill levels.

Event	Description	Container (kg)	Vessel Water (kg)	Vessel Volume (L)
Initial Weight	--	19.64	--	--
1st Pour	Free volume in fuel region	15.17	4.47	4.48
2nd Pour	Total, free volume in PV	14.47	5.17	5.18

For bulk fluid filling, about 4.60 kg of fluid was weighed in a fill container using a Mettler Toledo MS12002TS precision balance (repeatability 0.01 g) and a tared container. This value of 4.60 kg was chosen to be between the 4.47 kg needed to fill to the top of the fuel surrogate rods and the 5.17 kg that would fill the entire pressure vessel. This value would also allow for some losses during vessel filling while still attaining a fluid level above the rods. To fill the PV with fluid, the PV was pumped down to full vacuum, the flexible hose was submerged in the weighed fluid, and the fill/drain valve was opened to pull fluid into the PV.

For bulk fluid draining, helium at 140 kPa was allowed to enter the head space of the pressure vessel to serve as a cover gas while the fill/drain valve was opened to drain the fluid from the vessel. To scale the drain period from the HBDP cask down to the volume of the DDA vessel, the fill/drain valve was partially opened to achieve a drain period of 5-10 minutes, compared to the 43-minute drain period observed during the HBDP drain step, to reflect the ratio of the DDA vessel height to the HBDP cask height of 1:7. The fill/drain valve was closed as soon as no more bulk fluid was seen exiting the vessel, which was characterized by the formation of helium bubbles in the fluid container. A blowdown end criterion was defined as when the test operators did not observe fluid for at least three successive blowdowns. The vessel was then isolated from the helium flow in order to utilize the helium for MS drying before sampling during the vacuum holds – this ensured that the water content measured in the MS was representative of remaining water in the vessel, rather than residual moisture in the tubing lines.

2.5 Boric Acid Preparation and Pre-Fill Fluid Characterization

To prepare the boric acid solution, the weight of the water was measured, then a molar balance calculation was conducted to determine the amount of solid boric acid to be mixed into the water to obtain a 0.2 M boric acid solution as seen in Equation 2-1. In this equation, W is the weight of water in pounds,

A is the weight of boric acid in grams, 0.2 is the molarity of the solution being created, and the rest of the constants are conversion factors.

$$\boldsymbol{A(g) = \frac{W\,(lbs)}{8.34\,(\frac{lbs}{gal})} * 3.78541\,(\frac{L}{gal}) * 0.2\left(\frac{mol}{L}\right) * 61.83(\frac{g}{mol})} \qquad \text{Equation 2-1}$$

Table 2-2 shows the corresponding measured weights of the water and the solid boric acid powder that were mixed together. A sample was taken for inductively coupled plasma optical emission spectrometry (ICP OES) analysis; the weight of this sample was subtracted from the solution to determine how much of the 0.2 M boric acid solution was left before filling the DDA.

Table 2-2 DDA measured initial boric acid solution for the DDA tests using 0.2 M boric acid.

Test Date	Weight of Water for Boric Acid Solution (kg)	Weight of Solid Boric Acid (kg)	Weight of Boric Acid Sample for Analysis (kg)	Weight of Boric Acid Solution Before Filling (kg)	Weight of Boric Acid Solution in Vessel (kg)	Volume of Boric Acid Solution in Vessel (L)
02/16/22	4.60	0.0569	0.03	4.62	4.60	4.60
03/02/22	4.59	0.0568	0.03	4.61	4.61	4.61

Upon adding boric acid to water, the reaction shown in Equation 2-2 occurs. H_3O^+ is known as the conjugate acid and $B(OH)_4^-$ is the conjugate base. Both acids and bases can corrode material, so ensuring most of the aqueous solution is removed in drying is top priority.

$$\boldsymbol{B(OH)_{3,s} + H_2O_l \rightarrow B(OH)_4^-{}_{aq} + H_3O^+{}_{aq}} \qquad \text{Equation 2-2}$$

Samples taken of the solution before the tests were tested for pH, density, and boron concentration; the results are shown in Table 2-3. Boron was analyzed using ICP OES. Each pre-DDA sample was diluted to a 1:100 ratio. Standards were made to test within a range of 50 ppm_m and 0.5 ppm_m. The ICP OES tested each sample three times and reported the average. The results were then multiplied by 100 and reported in Table 2-3. The measurement precision, which is given by the relative standard deviation (RSD), expressed as a percentage, is also reported in Table 2-3.

The measurement accuracy is reported by the correlation coefficient, R. The closer to the value is to 1, the better the standard and the more accurate the results. For boron, for the February samples, R = 0.999674; for the March samples, R = 0.999853.

Given a concentration of 0.2 M of boric acid, the expected boron concentration is ~2,200 ppm_m. The samples show elevated concentrations of boric acid, which are likely due to a combination of human and instrument error. As the results are multiplied by 100, since the samples were diluted to a 1:100 ratio, that error propagates. Other errors could have resulted from the accuracy of the scale used to measure the boric acid and from some cross contamination with pipette usage. However, as stated previously, concentrations higher than 2,200 ppm_m are often used in SFPs, so the data is still representative. The slightly elevated acid concentration also serves as a conservative measure for potential corrosion of the material.

Table 2-3 Analysis of pre-DDA fill boric acid solution samples.

Sample ID	pH	Density (g/mL)	Boron (ppm_m)	Boron RSD (%)
02/15 Pre-DDA Fill	4.73	1.00	2,740	0.33
03/01 Pre-DDA Fill	4.79	1.00	2,730	0.98

2.6 Instrumentation

This section will describe the instrumentation used to measure temperature and pressure during this test series, as well as instrumentation specific to moisture/water content measurement.

2.6.1 Thermocouples

Temperatures were measured using type-T thermocouples using the standard ASTM calibration specifications (ASTM, 2017). No additional calibrations were performed. A coordinate system was defined with an origin ($z = 0$) at the top of the bottom nozzle on the sub-assembly, where the rectilinear z-coordinate runs along the axial length of the pressure vessel towards the upper blind flange (see Figure 2-6). The thermocouples installed along the surfaces of the fuel rod surrogates (internal TCs) are shown in Table A-1 in Appendix A with their data acquisition (DAQ) labels, while ambient TCs and those installed on the surface of the pressure vessel (external TCs) are listed in Table A-2. The 0° angular direction is defined as the side of the PV pipe near the strapping point on the mount. For the fuel rods, the 0° direction maintains this downward-facing (-z) reference for defining the clockwise direction.

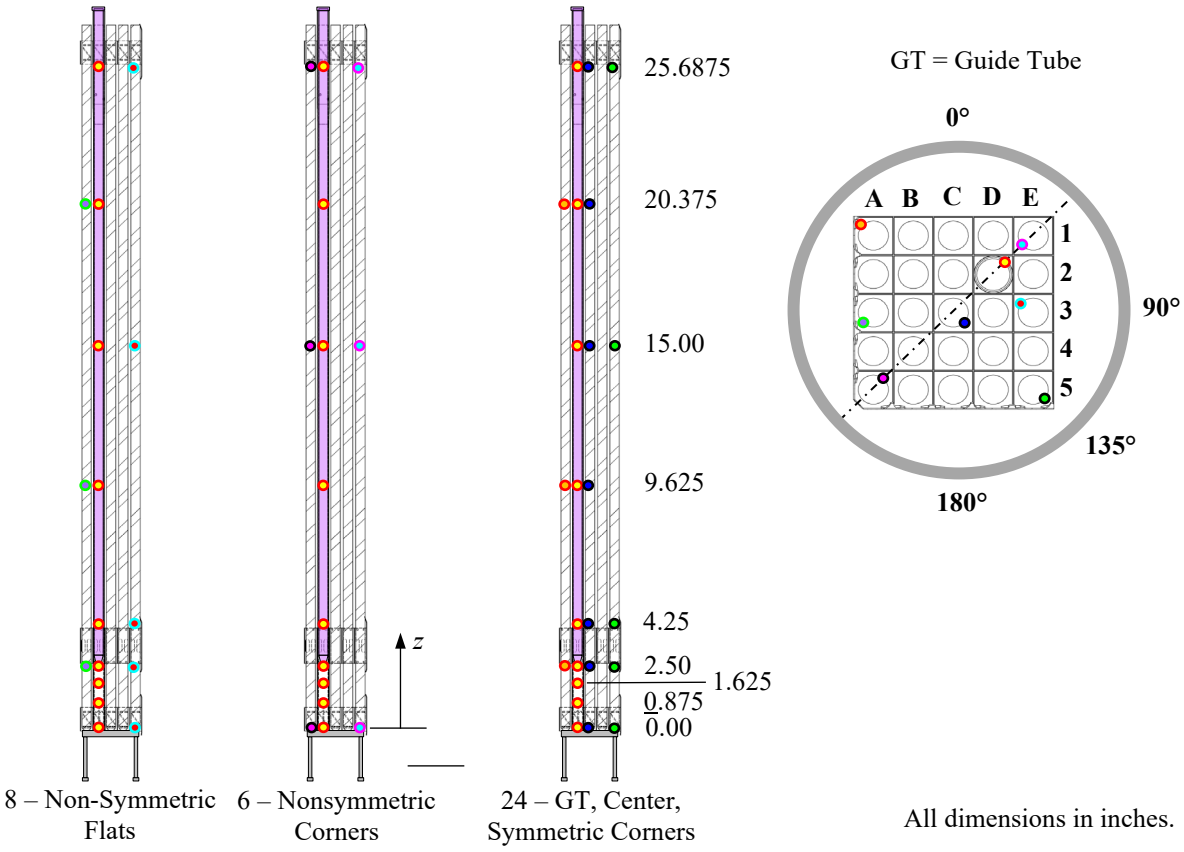

Figure 2-7 Diagram of thermocouple locations and assembly coordinate system.

The type-T TCs are intended to detect the presence of water by measuring sharp temperature changes that would be indicative of phase change during the vacuum drying procedure. The effective measurement range of type-T TCs runs from -270 to 400 °C. Under vacuum, the vapor pressure of the water inside water-retaining cavities will decrease and allow water to evaporate. As the rate of evaporation increases with decreasing pressures, the liquid temperature drops through evaporative cooling. Freezing may also occur if the enthalpy of fusion is exceeded near areas of restricted flow.

The external TCs in Table A-2 in Appendix A are type-T and installed along the axial length of the pressure vessel at 0°, although some additional TCs are installed at 90°, 135°, and 180° as well. The ambient thermocouples are installed on the left side of the upright fixture table installation behind the pressure vessel (see Figure 2-7).

2.6.2 Pressure Measurement and Control

Multiple transducers are employed to provide data for various pressure ranges during the drying test. They are installed external to the PV on VCR fittings and separated with a series of isolation valves until measurement is needed.

An MKS Model 627F heated capacitance manometer rated at 1,333 kPa (10,000 Torr) is employed as an absolute pressure transducer. This manometer is meant to provide overarching pressure measurement for backfill pressurized operations (222 kPa) and vacuum operations (100 mTorr) in the pressure vessel. The corrosion- and fouling-resistant Inconel sensor measures pressure directly (independent of gas composition) and is maintained at a temperature of 45 °C after a warm-up period of 4 hours. The instrument has a resolution of 0.001% full-scale (FS) and accuracy of 0.12% of reading, and it is calibrated with a traceable reference standard. Measurements below 100 Torr were relegated to two additional vacuum transducers for higher accuracy.

Three Setra Vactron Model 760 capacitance monometers were used as absolute pressure transducers for operations under low vacuum. Among the three transducers, two full-scale ranges of 1.33 and 13.3 kPa (10 and 100 Torr) were used, with resolutions of 0.01% FS, accuracies rated to ±0.15% of reading, and calibrations with standard traceable to the National Institute of Standards and Technology (NIST). This implies a minimum pressure measurement of 0.013 Pa (1 mTorr) for the test series as limited by the 1.33 kPa (10 Torr) manometer. One Setra 100 Torr transducer and one Setra 10 Torr transducer are mounted vertically in a shared cross with the MKS transducer that is isolated from the pressure vessel via a bellows-sealed valve. The other Setra 100 Torr transducer was also mounted vertically but on the vacuum line to check for consistency with the transducer on the pressure line while both were open to the pressure vessel at 100 Torr or below; this transducer was also used to assist with drying out the MS line that operates between 10-100 Torr. The distance from the top flange and sample line heaters provided by this location mitigates the operating temperature constraint of 50 °C. Given proof pressures of 310 kPa (45 psia), the instruments were able to be exposed to the PV during the 160 kPa (23.2 psia) blowdown steps.

A Setra Model ASM high-accuracy pressure transducer is used to monitor pressure while backfilling the PV for drainage and blowdown. It has an accuracy of ±0.05% over a 345 kPa (50 psia) FS range, or ±0.10 kPa (±0.025 psia), and was calibrated to a primary standard traceable to NIST. The instrument interfaces with the pressure vessel via a pressure train leading from the top blind flange, which is separated from the manifold holding the main vacuum transducers. This branch includes a pressure relief valve, and it is isolated during vacuum drying tests to reduce leakage.

An Alicat Scientific PC-series single-valve pressure controller was used to set the fill pressure imparted to the pressure vessel from the helium cylinder. This controller has a NIST-traceable calibration to ±0.125% accuracy of the 1,034 kPa (150 psia) FS, with an operating range down to 0.5% FS. Repeatability of setpoint is specified at ±0.08% FS.

An Alicat Scientific MCW-series low pressure drop mass flow controller was added to the MS line to allow greater control over the drying gas flow rate, which facilitated drying of the MS sampling lines. This controller has a NIST-traceable calibration to ±0.1% of reading or ±0.1% of the 1 SLPM full-scale repeatability (whichever is greater), with an operating range down to 0.5% FS. Repeatability of setpoint is specified at ±(0.2% of reading + 0.02% of full scale).

2.6.3 Water Content Measurement

Mass spectroscopy is a nontraditional method for measuring the relative moisture concentration in gas (i.e. ppm_v). In mass spectroscopy, a small sample stream (1 to 20 scm^3/min, where scm^3 is a cubic centimeter of gas referenced at a standard temperature and pressure, depending on sample pressure) is ionized and drawn into a vacuum chamber through a quadrupole filter that influences how ionized species interact with the ion detector. Because mass spectroscopy draws a small sample flow, perturbations of the system pressure may be expected. Furthermore, adsorption and desorption of water on the small-bore stainless steel or glass capillary sample tubes can be an issue, especially as the sample flow rate drops with falling sample pressure. Heating the sample lines and quadrupole minimizes the problem, but it will still take several minutes of sample flow for equilibrium to be reached. For slowly changing transient operations expected in drying operation, the anticipated lags are expected to be manageable. With a properly designed inlet, the high temperature and the wide range of pressures inside the pressure vessel can be accommodated.

The Hiden Analytical HPR-30 is a 6 mm quadrupole MS with a Faraday cup detector employed to analyze transient gas concentrations in gas samples from the pressure vessel obtained via a stainless-steel capillary tube with 0.173 in. (0.439 cm) inner diameter at two pressure ranges. This HPR-30 MS was used in previous testing (Salazar *et al.*, 2020), but the system was modified to allow for sampling between 10 and 100 kPa (1.45 to 14.5 psia) and between 1.33 and 13.3 kPa (10 to 100 Torr). The high-pressure range of 10 to 100 kPa (1.45 to 14.5 psia) was used for drying out the MS with nitrogen and establishing a helium sampling background. A low-pressure range of 1.33 to 13.3 kPa was used for vacuum drying tests.

The MS, shown in Figure 2-8, uses a scroll pump in combination with a turbo molecular pump to evacuate the internal volume and reduce the pressure within the spectrometer. This allows sample gases to flow into an ion source, which ionizes the molecular components of the sample gas.

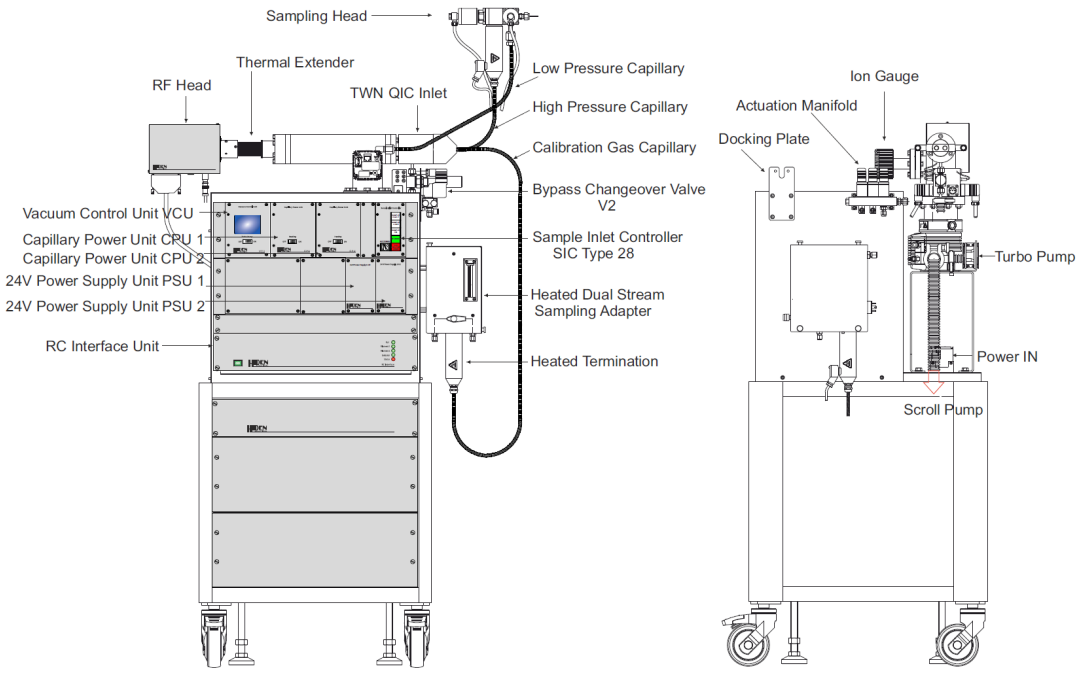

Figure 2-8 Hiden Analytical HPR-30 mass spectrometer system with a QIC dual-stage sampling head for measuring water content from the waterproof heater rod pressure vessel (Hiden Analytical Limited, 2018).

The ionized molecules are guided by a potential gradient between the ion source and ground to a quadrupole, which filters the molecules based on their mass-to-charge ratio *m*/*z* (amu/Coulomb). The quadrupole influences how the charged molecules are detected by the Faraday cup – the MS outputs the number of counts of ion-detector collisions based on *m*/*z*. The relative concentrations of each molecular component can thus be calculated from the ion detector collision count peaks at each *m*/*z* value.

A given gas sample will have multiple peaks based on how the molecules are ionized (singly or doubly charged) and the presence of molecular isotopes. For each molecule, determining a relative concentration amounts to accounting for the major peak of that molecule, which is associated with the molecule's most common ionic species. For example, as shown in Figure 2-9, the three peaks associated with nitrogen come from singly-charged $^{28}N_2$ (28 amu/1 C = 28 amu/C), doubly-charged $^{28}N_2$ (28 amu/2 C = 14 amu/C), and singly-charged $^{29}N_2$ (29 amu/1 C = 29 amu/C). The 28 amu/C peak is the largest peak in the mass spectrum of nitrogen, so it is the peak used for quantification. Since the drying process is transient, a rapid method was needed to resolve temporal changes and only the major peaks for water, helium, nitrogen, oxygen, and argon were analyzed. For the boric acid tests, byproducts of the reaction of boric acid with water were also included in the MS analysis; however, these byproducts remained in solution and were not detected in the gas phase. The resulting scan rate for the method developed was about 60-90 seconds per scan, with the scan rate directly affected by the number of molecular compounds being scanned.

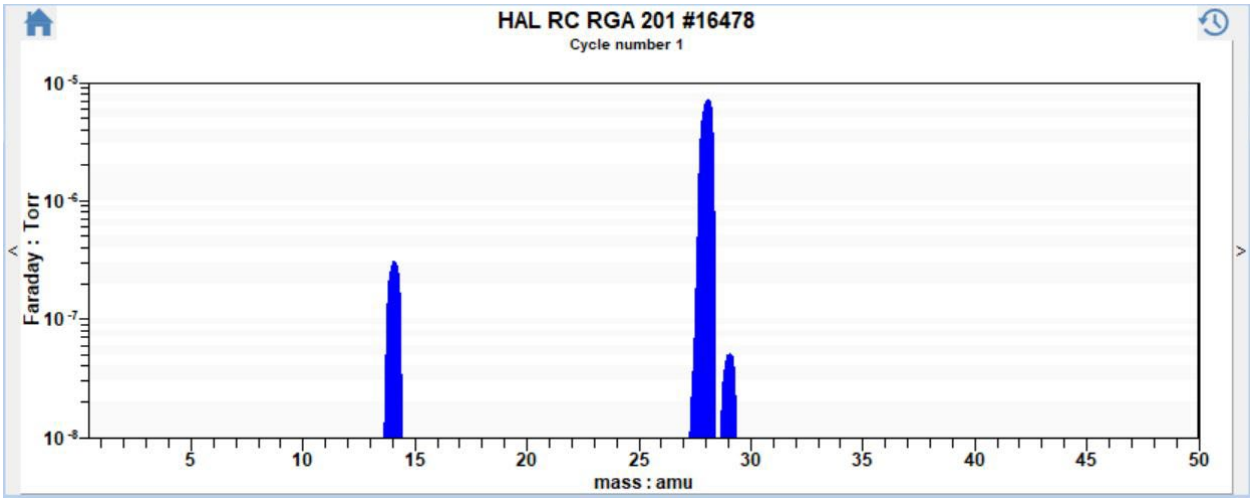

Figure 2-9 Mass spectrum of air showing the major peaks for nitrogen.

The amount of residual water detected will help define the effectiveness of the drying procedures implemented. An advantage of using an MS is that all other gaseous species are analyzed. For vacuum drying, the amount of air components can be used to evaluate the air leakage into the system. If used to monitor a commercial dry cask, an MS can also detect hydrogen generation that would indicate radiolysis or noble gas fission products (e.g. Kr-85 or Xe-137) that would indicate a leaking fuel rod.

The MS was calibrated to detect water content using a Michell DG2 two-stage dew point (DP) generator (-40 °C to +20 °C dew points). The generator uses a dry gas source such as ultra-high purity helium or air and generates a split stream that is mixed with moisture at a controlled temperature to generate a gas with a known dew point between -40 °C to +20 °C. The dew point of the calibration gas was verified by passing through a Michell S8000 chilled mirror hygrometer that can provide precision measurements to -65 °C dew point. The MS was calibrated for moisture concentrations between zero and 25,000 ppm_v using helium as the background gas. The calibration procedure was used to generate a relative sensitivity factor for water that is used to calibrate the MS water content measurements to the chilled mirror hygrometer measurements. This calibration procedure is described in greater detail in the FY20 waterproof heater rod testing report (Salazar *et al.*, 2020).

The result of the calibration conducted for this test series is shown in the linear regression in Figure 2-10. The relative sensitivity factor was calculated to be 0.2137, taken from the slope of the linear regression. The intercept was previously defined as the detection limit of the MS. However, the apparent outlier at the high ppm_v water content may have affected the regression calculation, resulting in a negative intercept. The linear regression had a coefficient of determination of $R^2 = 0.9971$ and a standard error of 36.1 ppm_v. The 95% confidence interval for the regression, based on the *t*-statistic of 1.975 and the standard error, was ±71.3 ppm_v. The standard deviation of the difference between the corrected HPR-30 and S8000 data was ±169.0 ppm_v.

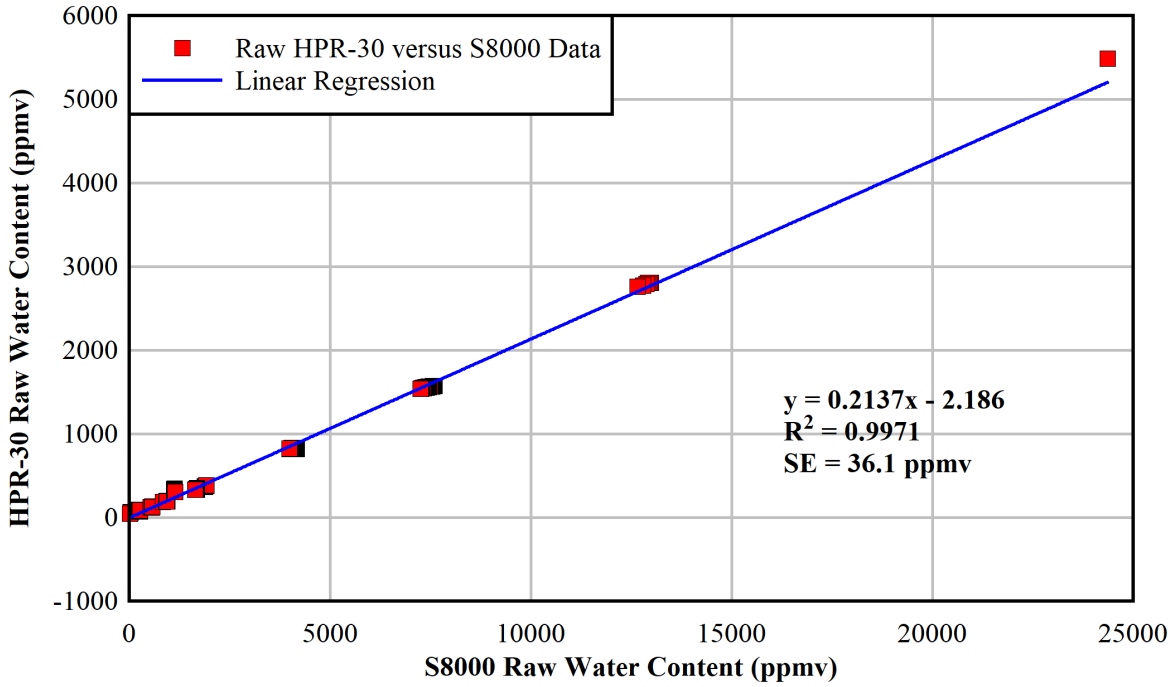

Figure 2-10 Linear regression for determining the relative sensitivity factor for water in a helium background when calibrating the HPR-30 mass spectrometer with respect to the S8000 chilled mirror hygrometer.

2.7 Power Control

The electrical power supplied to each heating element on the pressure vessel was controlled using four digital silicon-controlled rectifiers (SCR) labeled A through D. These were used to maintain the desired temperatures in the PV and guide tube and to have them remain within safe operating margins. The device software provided digital power setpoints to each SCR that was controlled based on external power feedback from a calibrated diagnostic unit (APlus) installed on the 120 VAC power supply. Diagnostic measurements from the APlus were available from SCRs A – C by connecting their power lines to the three available ports. On-board power information from SCR D was fed directly to the DAQ.

Table 2-4 lists the instruments used for power control and measurement, and Figure 2-11 shows the power control setup. Given the 627 W rating and 219 °C temperature limit of the flexible heaters, 10-amp fuses were installed in the circuit in the event that the heaters shorted during the tests. The full-scale settings for SCR control were defined as 1,000 watts, 120 volts, and 8.333 amps. The SCRs shared the same ground as the power source. A power conditioner was used to stabilize the power signals to the SCRs and impart more predictable power fluctuations during the test.

A flexible heater was installed in the MS inlet line (the purple line in Figure 2-6) and was controlled manually using a built-in control panel. This was done to reduce the potential for moisture condensation and maintain a representative PV sample.

Table 2-4 List of power control equipment.

Description	Manufacturer	Model
Digital SCR AC Power Controller	Control Concepts	uF1HXLGI-130-P1RSZ
Power Monitor with System Analysis	Camille Bauer	APlus
24 VDC Power Supply	Black Box	MDR-60-24
Power Conditioner	Eaton	PowerSure 800
Flexible Heaters with Stripped Leads	Omega	SRT202-060LSE
Flexible Heater with Percentage Controller	Omega	HTWC101-006

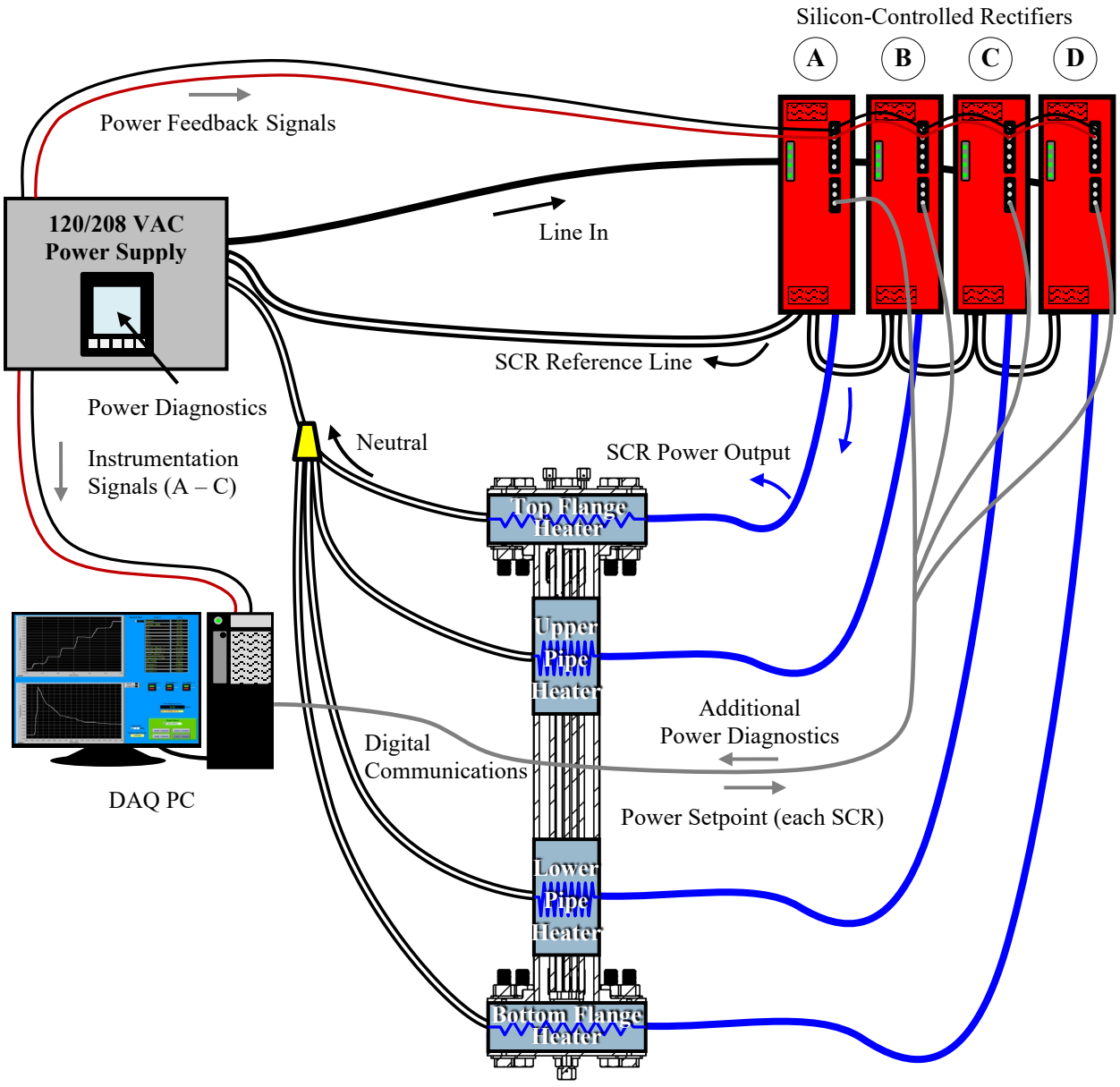

Figure 2-11 Diagram of the power control setup for the external heaters on the PV.

This page is intentionally left blank.

3 PRELIMINARY TEST RESULTS

3.1 Data from the High Burnup Demonstration Project

The temperature and pressure history for the drying and backfill portions of the HBDP was used as guidance for operating the DDA during testing. Figure 3-1 shows the temperature (top) and pressure (bottom) histories of the HBDP. The relative axial position of the temperature data labeled in the legend are shown by matching colored lines overlain on the inset HBDP vertical cross-section. Transient pressure data was not available to the authors. The pressure history presented in the plot was reconstructed from the available description and details as recorded in the High Burnup Test Report (EPRI, 2019). No details were provided on vacuum hold points during the vacuum drying procedure. This procedure is therefore represented as a dashed straight line between known pressures at the start and end of the drying procedure. The dryness test started at a pressure of 0.055 kPa (0.041 Torr) at 13.8 hours and rebounded to 0.13 kPa (0.97 Torr) after 30 minutes. The cask was then backfilled with helium to 102 kPa then evacuated to 10 kPa before finally being backfilled with helium to 222 kPa.

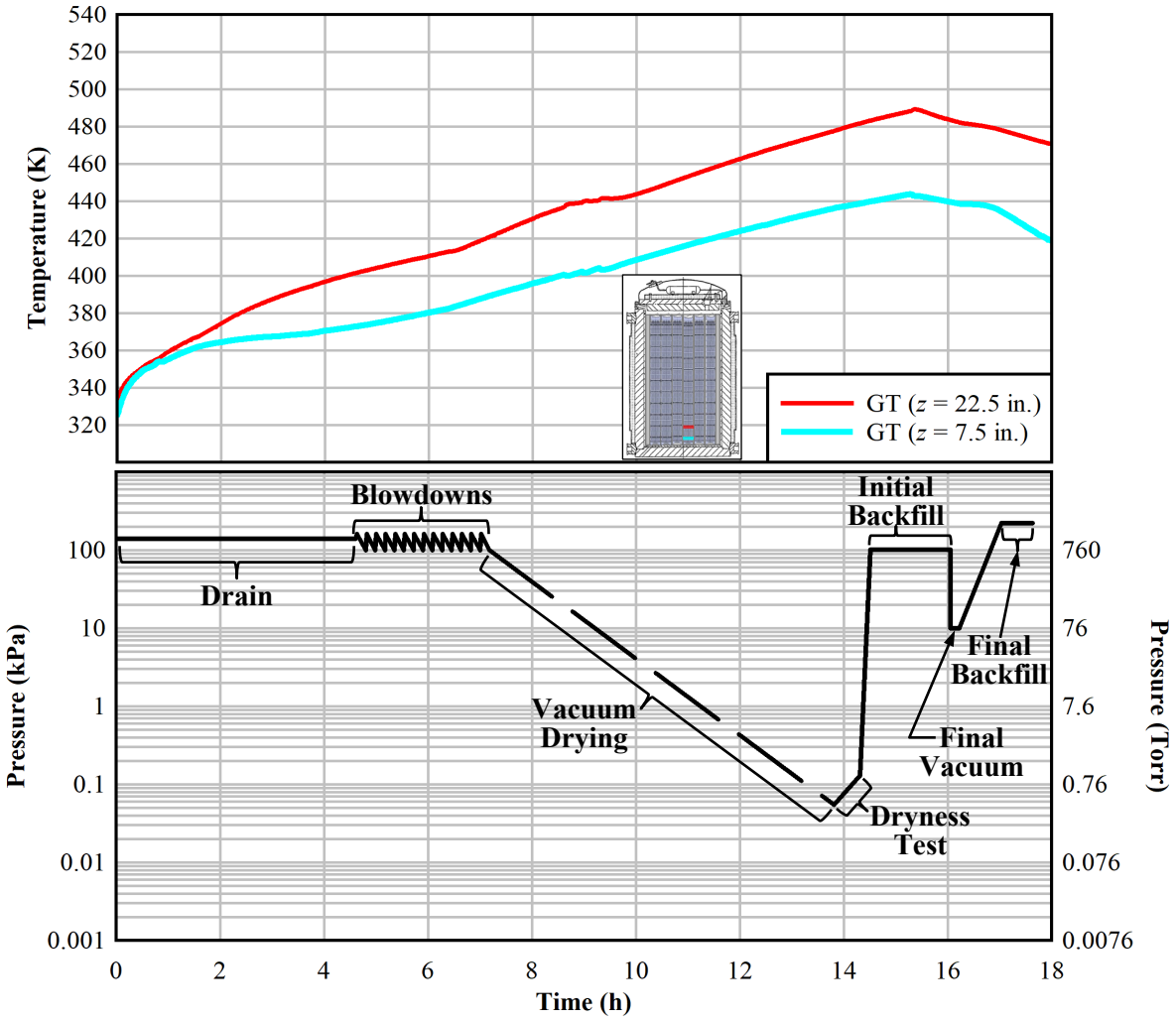

Figure 3-1 Temperature (top) and pressure (bottom) histories during drying of the High Burnup Demonstration Project.

The peak temperature at the upper portion of the region of interest (z = 22.5 inches) was a bit over 480 K and the peak temperature at the lower region (z = 7.5 inches) was just over 440 K. The time for performing the entire drying operation for the HBDP was just under 18 hours. These temperature and pressure histories from the HBDP serve as the template for the testing with the DDA described in the next section.

3.2 DDA Temperature and Pressure Histories

Figure 3-2 shows the corresponding temperature (top) and pressure (bottom) histories of the DDA during the drying test conducted on February 8, 2022, using deionized water as the fill fluid. The overall time scale is compressed by approximately a factor of two compared to the HBDP shown in Figure 3-1. The relative axial position of the temperature data labeled in the legend are shown by matching colored lines overlain on the inset DDA vertical cross-section. Before this test, a baseline pressure vessel leak rate, which was established upon confirmation that the vessel was as dry as possible before filling the vessel with water, was measured to be 7 millitorr per minute.

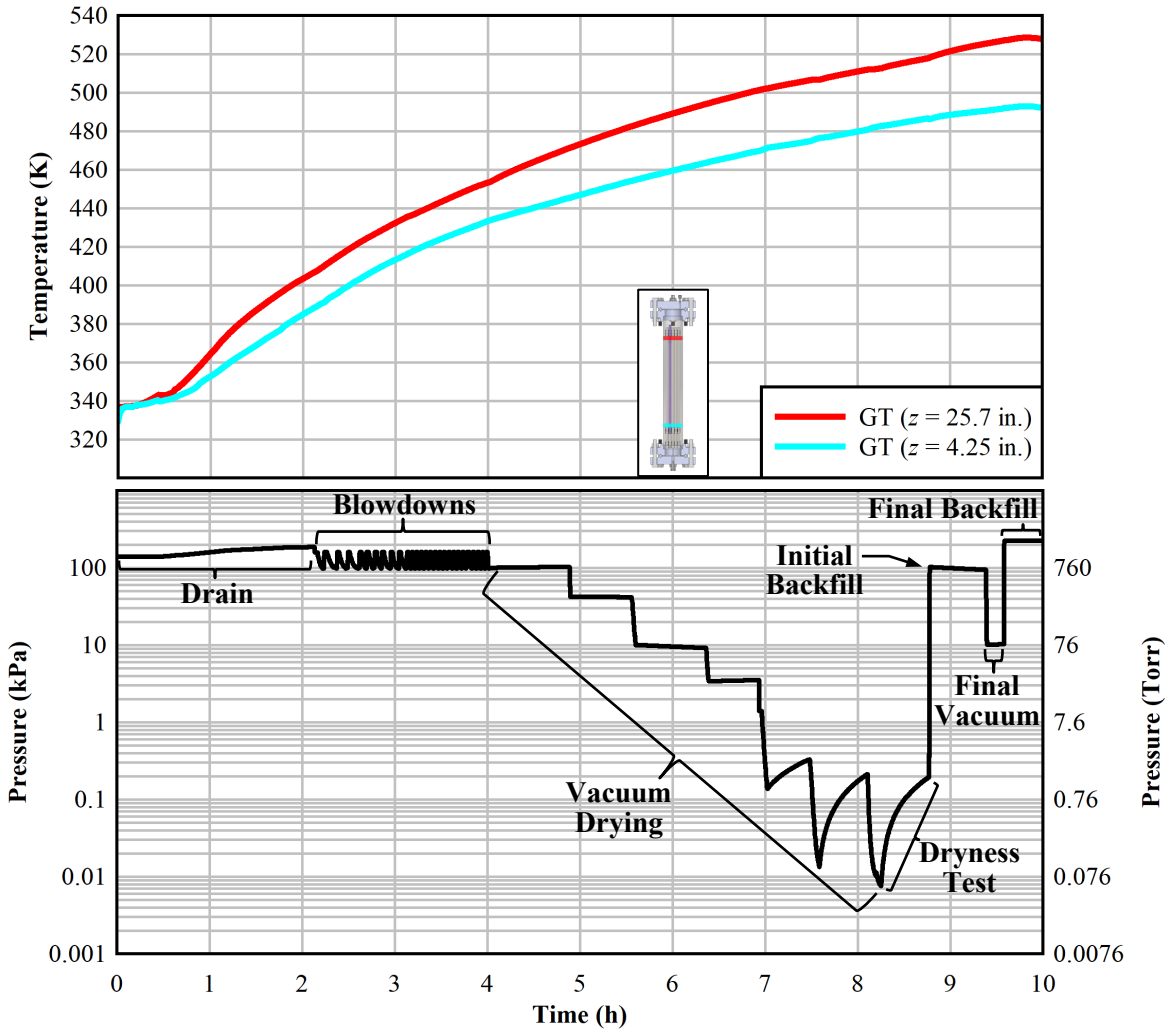

Figure 3-2 Temperature (top) and pressure (bottom) histories during simulated drying of the DDA with an open guide tube and deionized water on 02/08/22.

The transient pressure data in Figure 3-2 shows all the details of the 02/08/22 DI water test progession. The elapsed start time shown in the plot corresponds to the beginning of the drain step. The increase in pressure seen in the drain step was due to isolation of the pressure vessel and the corresponding rise in pressure from the rise in temperature of the internal volume. A total of twenty-eight blowdowns were needed for the operators to no longer observe water exiting the vessel after three successive blowdowns.

The peak temperature at the upper portion of the region of interest (z = 25.7 inches) was 529 K and the peak temperature at the lower region (z = 4.3 inches) was 493 K. The time for performing the entire operation was about 10 hours. Overall, the peak temperatures seen in the DDA test were about 50-55 K higher than the HBDP results due to the extended blowdown period extending the overall test time by 1 hour. However, the overall temperature profiles as a function of time were very similar. The corresponding temperatures up to the 7.5 hour elapsed time mark were about 20-30 K higher in the upper guide tube region and between 20 to 40 K higher in the lower guide tube region than the HBDP temperatures. Unlike previous testing, the power supplied to the heaters remained constant during the entire blowdown and vacuum hold procedures. Therefore, any temperature changes in the profile during those steps can be more closely associated with changes in the internal environment. Such changes include the evaporation of residual water from internal surfaces or the introduction of helium, which would improve overall thermal conductivity and increase the heat flux away from the vessel.

Figure 3-3 and Figure 3-4 show the temperature (top) and pressure (bottom) histories of the DDA during the drying test conducted on February 16, 2022 and March 2, 2022, respectively, using an open guide tube and 0.2 M boric acid fill fluid that more accurately represents the fluid present in a spent fuel pool. The overall time scale is again compressed compared to the HBDP. The relative axial position of the temperature data labeled in the legend are shown by matching colored lines overlain on the inset DDA vertical cross-section. Before these tests, a baseline pressure vessel leak rate was established upon confirmation that the vessel was completely dry before filling the vessel with water. This leak rate was measured to be 0.45 millitorr per minute for the 02/16/22 test and 1.2 millitorr per minute for the 03/02/22 test.

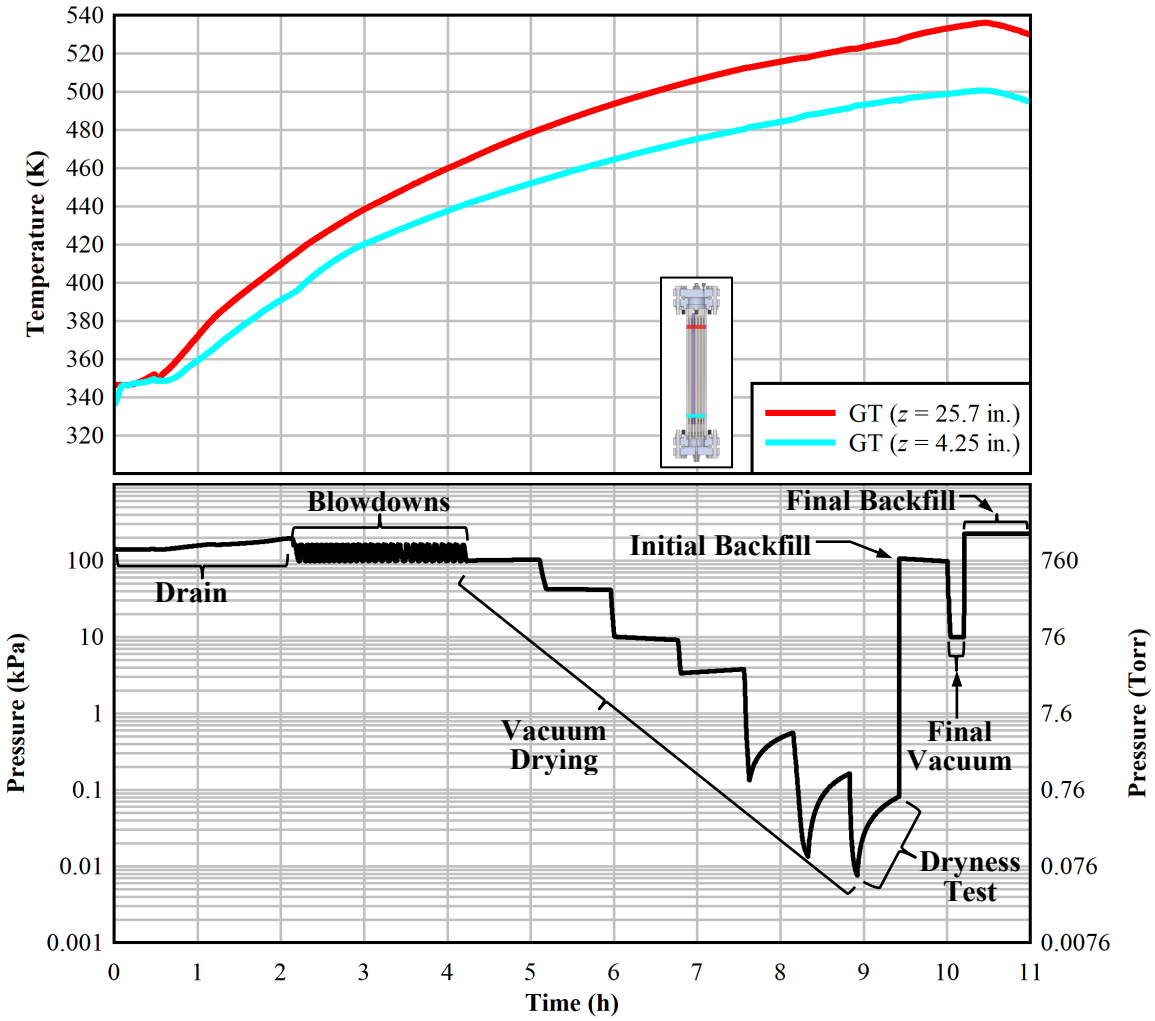

Figure 3-3 **Temperature (top) and pressure (bottom) histories during simulated drying of the DDA with an empty guide tube and 0.2 M boric acid on 02/16/22.**

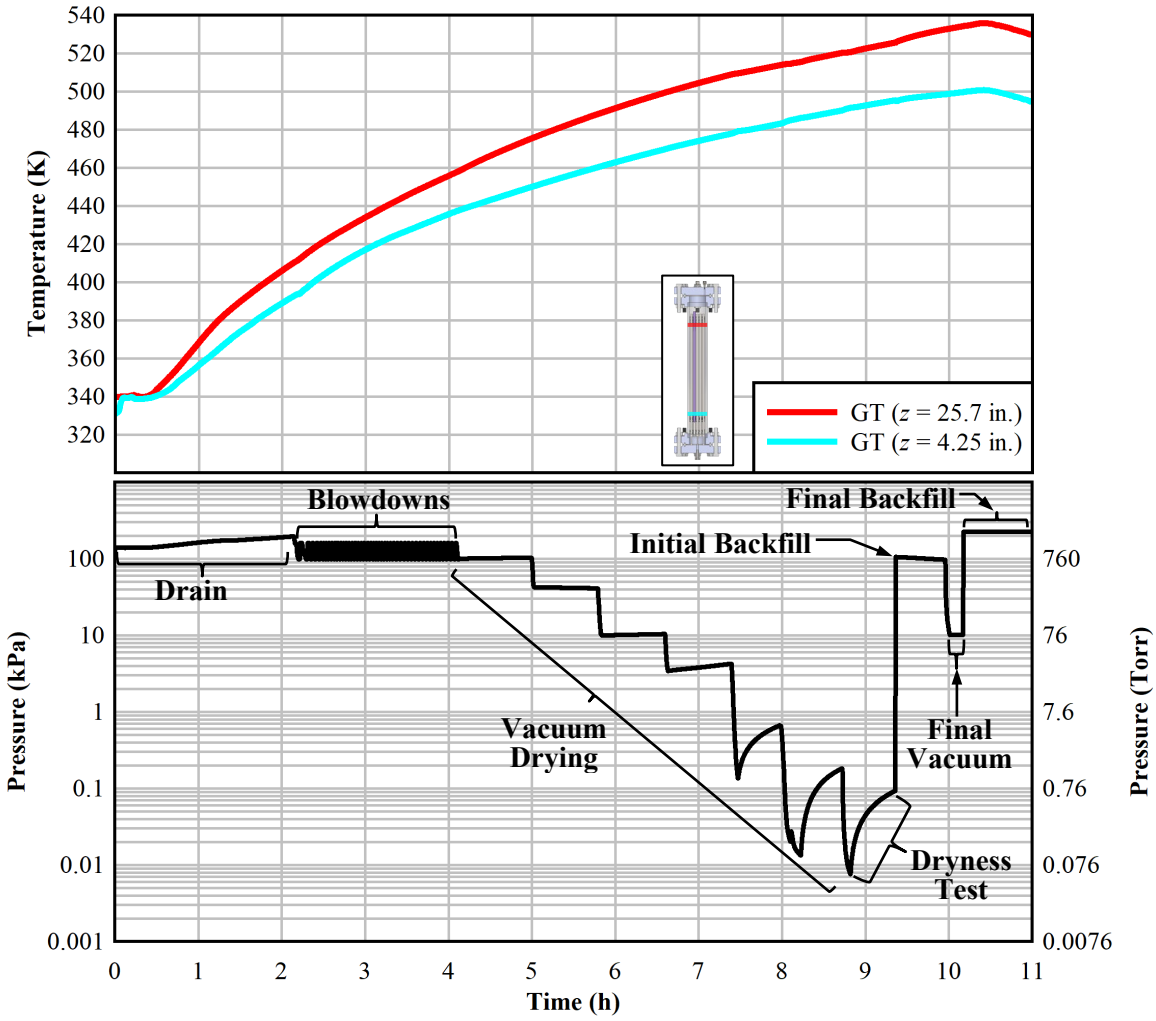

Figure 3-4 Temperature (top) and pressure (bottom) histories during simulated drying of the DDA with an empty guide tube and 0.2 M boric acid on 03/02/22.

The transient pressure data in Figure 3-3 and Figure 3-4 show all the details of the test progression in the 02/16/22 and 03/02/22 boric acid tests, respectively. The test start time is once again defined as the beginning of the drain step. For the 02/16/22 test, 28 blowdowns were conducted to match with the deionized water test, and at least three successive blowdowns occurred with no operators observing fluid exiting the vessel. Another boric acid test was run on 02/23/22 which demonstrated that 28 blowdowns was insufficient for evacuating all of the boric acid from the pressure vessel; however, due to instrumentation and DAQ issues during the test, the results are not included in this report. For the 03/02/22 test, 48 blowdowns were conducted to ensure that no more fluid was observed exiting the pressure vessel – the operators did not observe fluid exiting the vessel for at least thirteen blowdowns.

The peak temperature at the upper portion of the region of interest (z = 25.7 inches) was 536 K for both the 02/16/22 and the 03/02/22 boric acid tests. The peak temperature at the lower region (z = 4.3 inches) was 501 K for both the 02/16/22 and the 03/02/22 boric acid tests. The time for performing the entire operation for both tests was about 11 hours. Overall, the peak temperatures seen in the DDA test were about 55-60 K higher than the HBDP results due to the extended blowdown period extending the overall test time by 2 hours. However, the overall temperature profiles as a function of time were very similar. The corresponding temperatures up to the 7.5 hour elapsed time mark were about 30-40 K higher in the

upper guide tube region and between 40-50 K higher in the lower guide tube region than the HBDP temperatures for both boric acid tests.

Table 3-1 shows the vacuum isolation periods for the three DDA tests. The isolation periods at the 317 Torr, 75 Torr, and 26 Torr pressures were chosen to accommodate the mass spectrometer scan rate of 60-90 seconds per scan – five scans at steady state were needed for data analysis, so isolation periods of 45 minutes were decided upon to ensure steady state conditions during the last five scans. The 1 Torr and 0.1 Torr isolations were reduced to 30 minutes to compensate for the initial mass spectrometer hold periods in order to keep the vacuum drying period roughly a factor of two less than that seen during the HBDP.

Table 3-1 Vacuum isolation periods for the DDA tests. Test data highlighted in blue is from the DI water test; test data highlighted in green are from the boric acid tests.

Test Date	Test Step	Vessel Isolation Start Pressure (kPa)	Isolation Start Time (h)	Isolation Period (h)
2/8/2022	1st vacuum isolation	42.3	4.9	0.7
	2nd vacuum isolation	10.0	5.6	0.8
	3rd vacuum isolation	3.47	6.4	0.6
	4th vacuum isolation	0.130	7.0	0.6
	5th vacuum isolation	0.013	7.6	0.6
	Regulatory isolation	0.008	8.3	0.5
2/16/2022	1st vacuum isolation	42.3	5.2	0.8
	2nd vacuum isolation	10.0	6.0	0.8
	3rd vacuum isolation	3.47	6.8	0.8
	4th vacuum isolation	0.130	7.6	0.7
	5th vacuum isolation	0.013	8.3	0.6
	Regulatory isolation	0.008	8.9	0.5
3/2/2022	1st vacuum isolation	42.3	5.0	0.8
	2nd vacuum isolation	10.0	5.8	0.8
	3rd vacuum isolation	3.47	6.6	0.9
	4th vacuum isolation	0.130	7.5	0.7
	5th vacuum isolation	0.013	8.2	0.6
	Regulatory isolation	0.008	8.8	0.5

For the 02/08/22 DI water test, the final vacuum hold at 0.008 kPa (0.057 Torr) began vessel isolation at 8.3 hours and rebounded to 0.19 kPa (1.44 Torr) just after 8.8 hours. This amounts to a rebound rate of 69 millitorr per minute. Correcting for the baseline leak rate of 7 millitorr per minute gives a 62 millitorr per minute rebound rate that can be attributed to water evaporation. The vessel was then backfilled with helium to 102 kPa (765 Torr) and a post-drying MS sample was taken for 36 minutes. Following sampling from the MS, the vessel was evacuated to 10 kPa (76 Torr) and held for 10 minutes. The final backfill to 222 kPa was implemented at about 9.6 hours elapsed time.

For the 02/16/22 boric acid test, the final vacuum isolation at 0.008 kPa (0.057 Torr) started at 8.9 hours and rebounded to 0.082 kPa (0.62 Torr) at 9.4 hours. This amounts to a rebound rate of 19 millitorr per minute. Correcting for the baseline leak rate of 0.45 millitorr per minute gives a 18.6 millitorr per minute rebound rate that can be attributed to water evaporation. The vessel was then backfilled with helium to 102 kPa, evacuated to 10 kPa (76 Torr) and held for 10 minutes. The final backfill to 222 kPa was

implemented at about 10.2 hours, and the power supplied to the external heaters was reduced 10 minutes after the backfill to protect the test setup.

For the 03/02/2022 boric acid test, the final vacuum isolation at 0.008 kPa (0.057 Torr) started at 8.8 hours and rebounded to 0.087 kPa (0.65 Torr) at 9.3 hours. This amounts to a rebound rate of 19.8 millitorr per minute. Correcting for the baseline leak rate of 1.2 millitorr per minute gives a 18.6 millitorr per minute rebound rate that can be attributed to water evaporation. This is the same rebound rate for the final vacuum isolation seen in the 02/16/22 boric acid test – therefore, the 03/02/2022 boric acid test served to demonstrate repeatability of results given largely identical test parameters. The number of blowdowns between the tests differed, but the blowdown criteria of test operators no longer seeing fluid exit the vessel after at least three successive blowdowns as well as a blowdown period of ~2 hours was the same across the two tests. The vessel was then backfilled with helium to 102 kPa, evacuated to 10 kPa (76 Torr) and held for 10 minutes. The final backfill to 222 kPa was implemented at about 10.4 hours, and once again, the power supplied to the external heaters was reduced 10 minutes after the backfill to protect the test setup.

3.3 DDA Guide Tube Axial Temperatures

Figure 3-5 shows the evolution of guide tube temperatures over time during the drying test with an open guide tube and deionized water. The vessel interior is in a primarily conductive or radiative regime due to the pressures seen inside the vessel remaining below 200 kPa until the final helium backfill. In order to compensate for this regime and more closely mimic the temperatures seen at the top of the dashpot region in a dry storage cask, most power was applied to the top portion of the vessel. Nonetheless, the temperatures were observed to peak in the middle of the vessel, i.e., at the guide tube axial level of z = 15.0 inches.

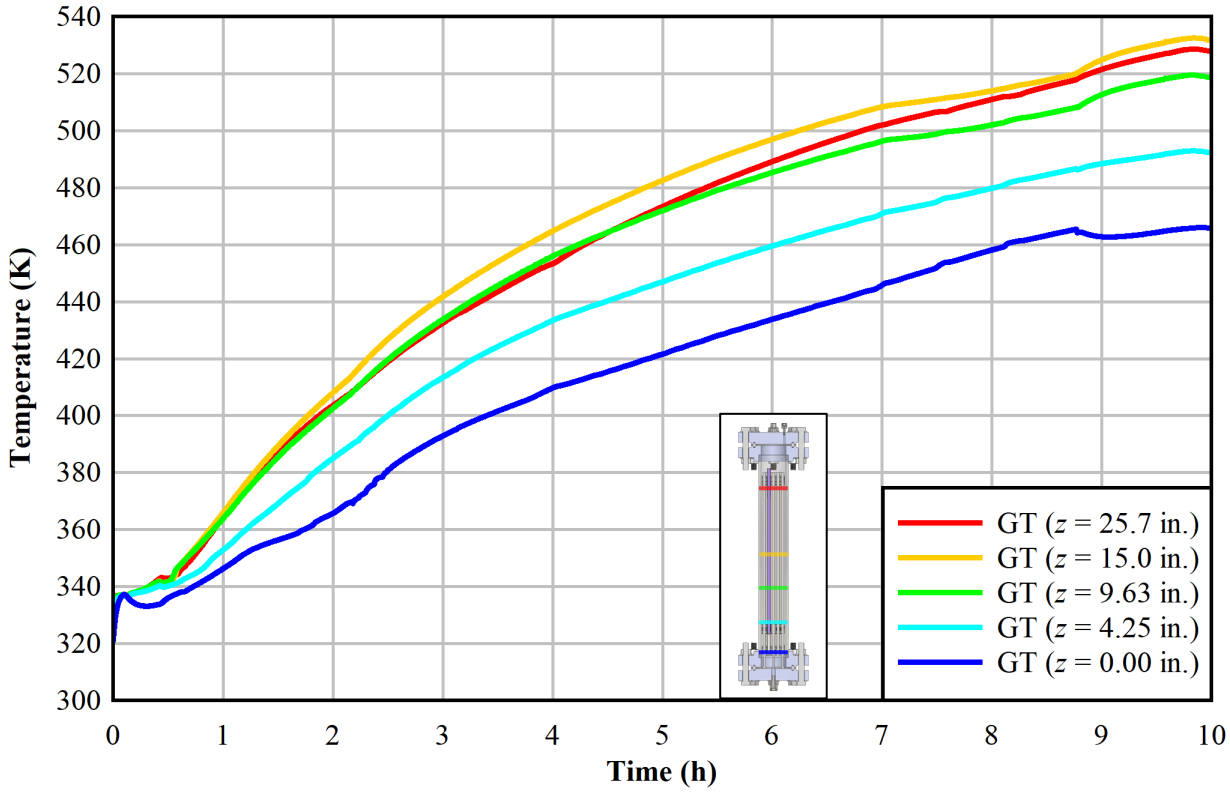

Figure 3-5 Guide tube temperatures versus time during simulated drying of the DDA with an open guide tube and deionized water on 02/08/22.

The peak temperature at the upper portion of the region of interest (z = 25.7 inches) was about 529 K and the peak temperature at the lower region (z = 4.3 inches) was about 493 K. The temperature trends are similar to what was seen in previous DDA testing with an empty guide tube (Durbin *et al*., 2021) in that there are no temperature drops associated with water evaporation into the internal volume. The open guide tube has a reduced number of water retention sites compared to a guide tube with a poison rod surrogate insert, so this behavior is expected. The constant power supplied to the heaters served as an improvement over previous testing, since the effects of helium backfill on the temperature trend can be seen at 8.8 hours. The effects of the thermal conductivity of helium can be seen by comparing the temperatures in the lower guide tube region to the temperatures in the upper guide tube region. The temperature drops at the z = 0 in., while the temperatures rise in the z = 9.6 in., 15.0 in., and 25.7 in. axial levels. This corresponds to edge effects associated with helium circulation in the vessel, with the hotter helium rising to the top of the vessel. This behavior differs from what was seen in the HBDP cask dashpot region, where both the z = 7.5 in. and z = 22.5 in. axial levels saw temperature drops upon the initial helium backfill, since the dashpot region in the DDA comprises the entire vessel, whereas the dashpot region in the HBDP cask only makes up approximately the lower fifth of the cask and thus undergoes behavior similar to the bottom portion of the DDA.

Figure 3-6 shows the evolution of guide tube temperatures over time, inserted for five elevations, during the 02/16/22 boric acid test; Figure 3-7 shows the same temperatures for the 03/02/22 boric acid test. Once again, most likely due to the pressures remaining below 200 kPa throughout the drying procedure and the edge effects typical of a primarily conductive regime, the temperatures saw a peak in the middle of the vessel, at the guide tube axial level z = 15.0 inches.

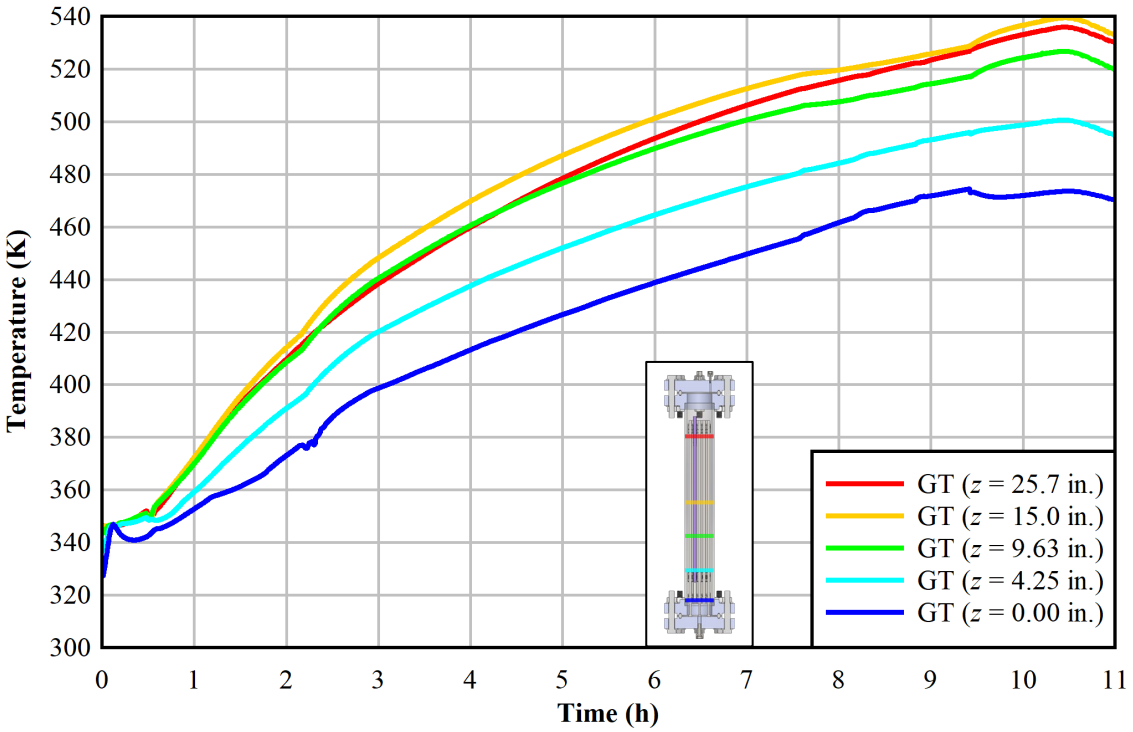

Figure 3-6 **Guide tube temperatures versus time during simulated drying of the DDA with an empty guide tube and 0.2 M boric acid on 02/16/22.**

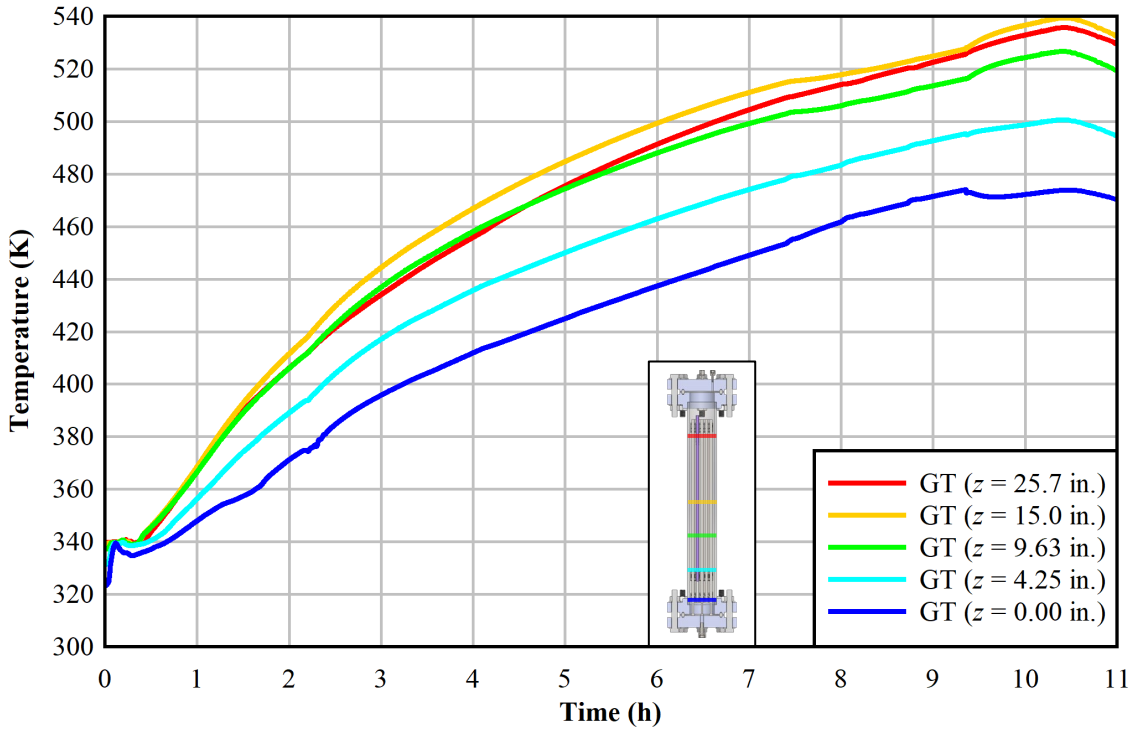

Figure 3-7 **Guide tube temperatures versus time during simulated drying of the DDA with an empty guide tube and 0.2 M boric acid on 03/02/22.**

The temperature trends are similar to what was observed in the 02/08/22 DDA test; however, for the 02/16/22 boric acid test at 2.15 hours and for the 03/02/22 boric acid test at 2.20 hours, small temperature drops associated with water evaporation were seen on the bottom of the guide tube (z = 0.00 in.). Once again, the effects of helium backfill on the temperature trends can be seen after 9 hours elapsed time. Similar to the DI water test, the temperature drops at the z = 0 in axial level, while the temperatures rise in the z = 9.6 in, 15.0 in, and 25.7 in axial levels for both boric acid tests, which again most likely occurs due to helium circulation.

For the 02/16/22 boric acid test, the peak temperature at the upper portion of the region of interest (z = 25.7 inches) was about 536 K and the peak temperature at the lower region (z = 4.3 inches) was about 501 K. The maximum temperatures in the upper and lower regions are within 8 K of the 02/08/22 DDA test with deionized water, which can be mostly attributed to the higher ambient temperatures at the start of the test (293 K versus 288 K for the 2/8/22 DI water test). The power supplied to the heaters was set to compensate for the higher ambient temperatures; regardless, the initial guide tube temperatures prior to the drain step for the 2/16/22 boric acid test were higher than for the 2/8/22 DI water test (327-346 K compared to 321-336 K), a 6-10 K temperature difference that encompasses the 8 K difference in maximum temperatures.

For the 03/02/22 boric acid test, the peak temperature at the upper portion of the region of interest (z = 25.7 inches) was about 536 K and the peak temperature at the lower region (z = 4.3 inches) was about 501 K. The maximum temperatures in the upper and lower regions are within 8 K of the 02/08/22 DDA test with deionized water and are identical to the maximum temperatures of the 02/16/22 DDA test with boric acid, once again demonstrating a repeat result using the same input parameters.

3.4 DDA Water Content Measurements

3.4.1 Post Drain/Blowdown Fluid Weights

Table 3-2 shows the weight of the measured initial fluid that was used to fill the DDA. It also shows the weight of the fluid recovered (plus the container) from the drain and helium blowdowns. The difference between the weight of the fluid before filling and after recovery from the drain and helium blowdowns gives a measure of the fluid remaining in the DDA after the helium blowdowns. These measurements indicate that there was about 10-20 mL (10-20 g) of fluid left in the vessel that needed to be removed by the vacuum isolations, which suggests that most of the fluid was removed following the helium blowdowns.

Table 3-2 DDA measured initial fluid content versus recovered fluid for determining fluid remaining in DDA after the helium blowdown procedure.

Test Date	Fluid Type	Weight of Fluid + Container Before Filling (kg)	Recovered Fluid + Container (kg)	Fluid Remaining in DDA (kg)	Fluid Remaining in DDA (L)
02/08/22	DI Water	4.60	4.59	0.01	0.01
02/16/22	0.2 M Boric Acid	4.60	4.58	0.02	0.02
03/02/22	0.2 M Boric Acid	4.61	4.59	0.02	0.02

3.4.2 Mass Spectrometer Measured Water Content

The MS has three independent inlets for sampling gas within three different pressure ranges. The three inlet sampling ranges were 100 to 10 kPa, 13.3 to 1.33 kPa, and 0.5 to 0.05 kPa. Since the pressure vessel was at 140 kPa during the drain step and rapidly changed between 160 and 100 kPa during the helium

blowdown steps, the MS could not sample from the pressure vessel during the drain and helium blowdown steps. Additionally, problems were encountered when attempting to sample the vessel at the lowest pressure using the 0.5 to 0.05 kPa sampling inlet. During the 03/02/22 boric acid test, the 13.3 to 1.33 kPa inlet pulled in a significant quantity of air, so the 100 to 10 kPa inlet was used to sample at the pressures between 1 and 10 kPa. In order to accommodate these constraints and provide a measure of dryness, cycling of the pressure in the vessel down to 100 kPa for sampling followed by pressurization with helium to the 222 kPa hold point continued for two more days past the "Final Backfill" step shown in Figure 3-2 through Figure 3-4.

Before each DDA test, the vessel is heated to ensure the internal volume exceeds 100 °C and a vacuum is applied to the vessel in order to dry the internal volume and ensure that any water sampled is from the water filling step. The MS lines are dried with nitrogen, then helium is used to purge the nitrogen out of the lines and define a baseline MS dryness level before introducing water. The measured water content from a typical dryness test is around 80 ppm_v.

The MS sampling results are summarized in Table 3-3. The water content data is presented in Figure 3-8 through Figure 3-10, while the dew point data is presented in Figure 3-11 through Figure 3-13. The first sample was taken at 42 kPa (317 Torr), the first vacuum isolation hold following the helium blowdowns. The second and third samples were taken at 9.9 kPa (75 Torr) and 3.5 kPa (26 Torr), respectively. The rest of the samples were taken during each helium backfill step, with the first backfill occurring immediately following the vacuum isolations and the second and third backfills occurring roughly 24 and 48 hours apart from the first backfill, respectively.

Table 3-3 Mass spectrometer water content data for the DDA tests. Test data highlighted in blue is from the DI water test; test data highlighted in green are from the boric acid tests.

Sampling Date	Test Step	High Pressure Hold, P_{Hold} (kPa)	Vessel Sampling Pressure P_{Sample} (kPa)	Predicted Water Content Based on Dilution Factor (ppm_v)	Measured Water Content (ppm_v)	Sample Pressure Dew Point (°C)
2/8/2022	1st vacuum isolation	--	42.3	--	2,761	-18.9
2/8/2022	2nd vacuum isolation	--	10.0	--	15,304	-16.8
2/8/2022	3rd vacuum isolation	--	3.47	--	53,087	-13.8
2/8/2022	1st helium backfill	102	102	--	739	-24.0
2/9/2022	2nd helium backfill	222	100	340	402	-30.7
2/10/2022	3rd helium backfill	222	100	153	306	-32.7
2/16/2022	1st vacuum isolation	--	42.3	--	10,383	-4.26
2/16/2022	2nd vacuum isolation	--	10.0	--	66,973	0.05
2/16/2022	3rd vacuum isolation	--	3.47	--	422,200	13.7
2/16/2022	1st helium backfill	102	102	--	920	-21.4
2/17/2022	2nd helium backfill	222	100	414	345	-32.2
2/18/2022	3rd helium backfill	222	100	186	234	-35.1
3/2/2022	1st vacuum isolation	--	42.3	--	6,916	-9.1
3/2/2022	2nd vacuum isolation	--	10.0	--	72,978	2.8
3/2/2022	3rd vacuum isolation	--	3.47	--	462,357	16.5
3/2/2022	1st helium backfill	102	102	--	1,155	-19.1
3/3/2022	2nd helium backfill	222	100	520	432	-30.1
3/4/2022	3rd helium backfill	222	100	234	303	-32.8

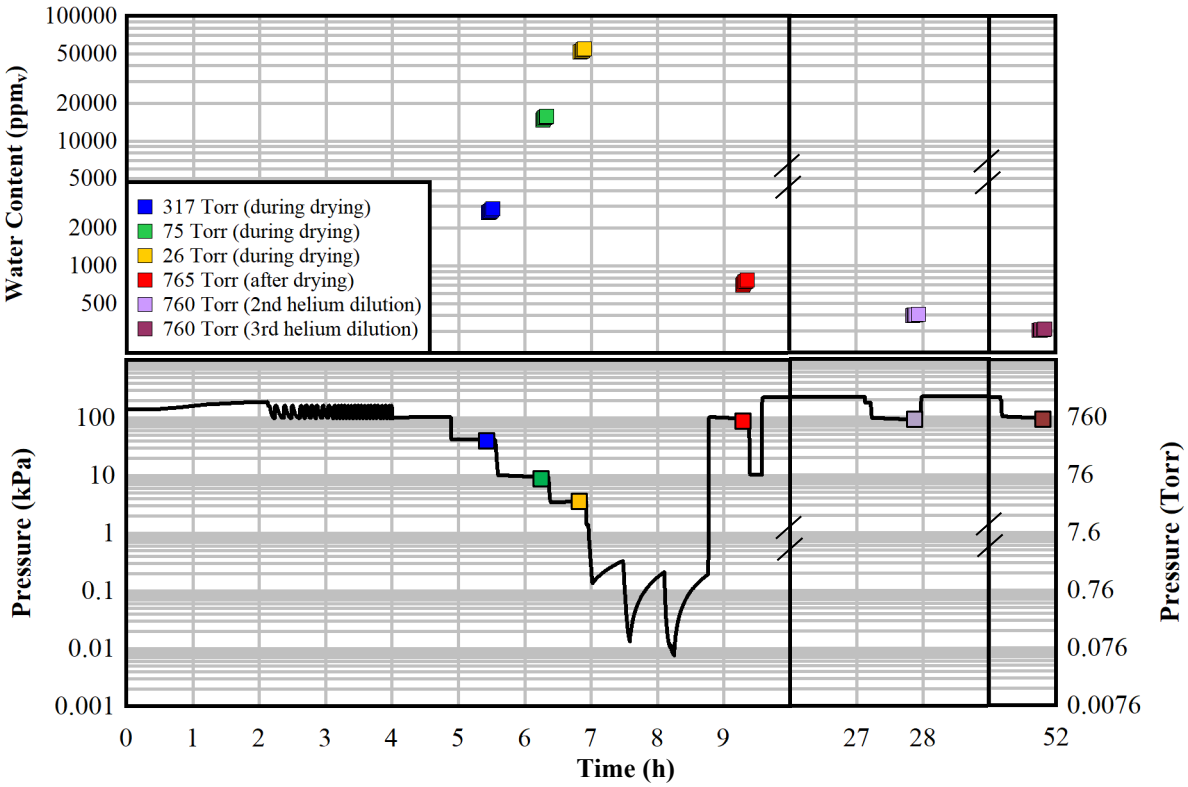

Figure 3-8 Water content measurements (top) and pressure (bottom) histories during simulated drying of the DDA with an open guide tube and deionized water on 02/08/22.

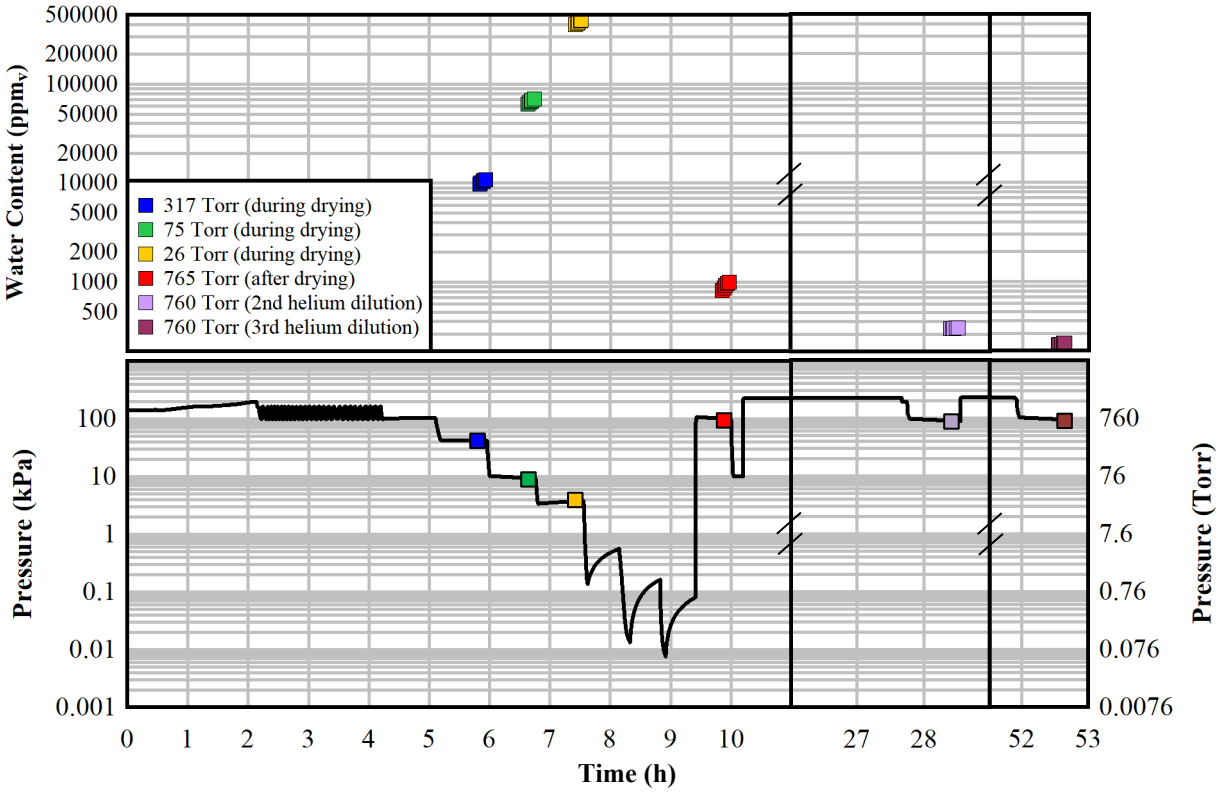

Figure 3-9 Water content measurements (top) and pressure (bottom) histories during simulated drying of the DDA with an open guide tube and 0.2 M boric acid on 02/16/22.

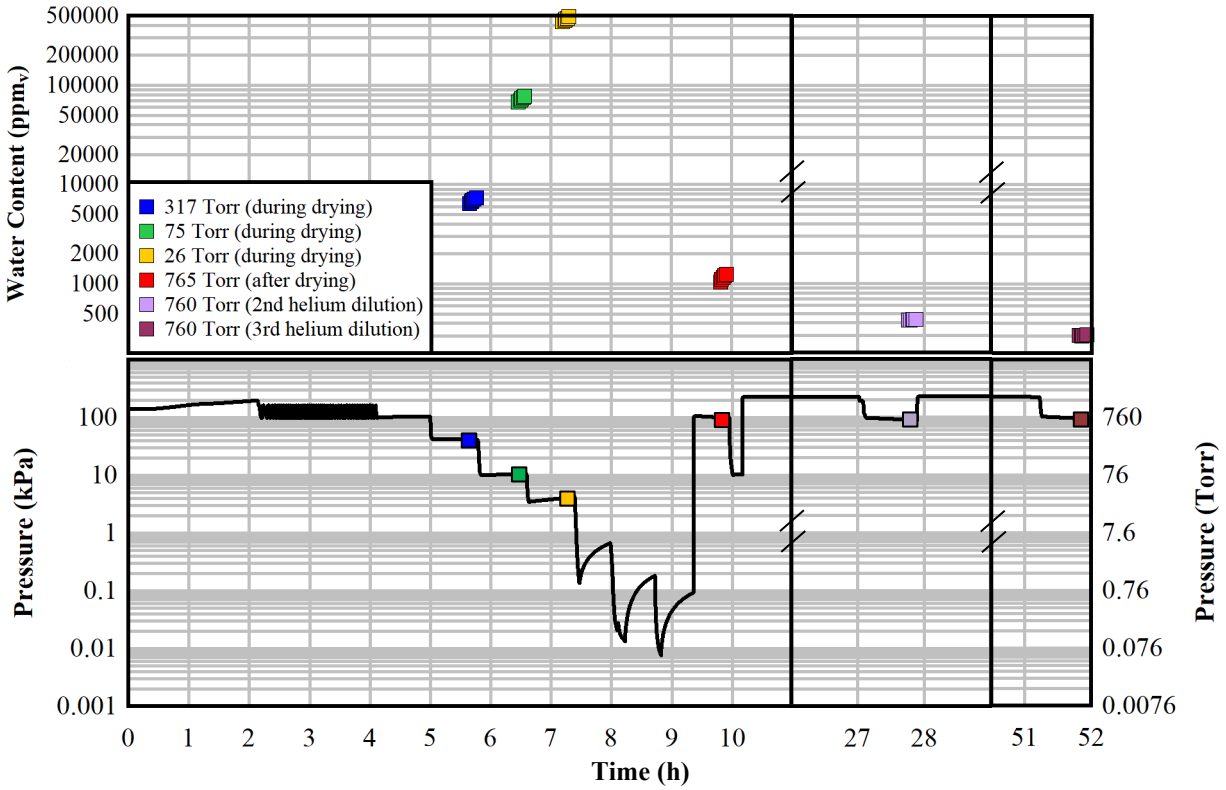

Figure 3-10 Water content measurements (top) and pressure (bottom) histories during simulated drying of the DDA with an open guide tube and 0.2 M boric acid on 03/02/22.

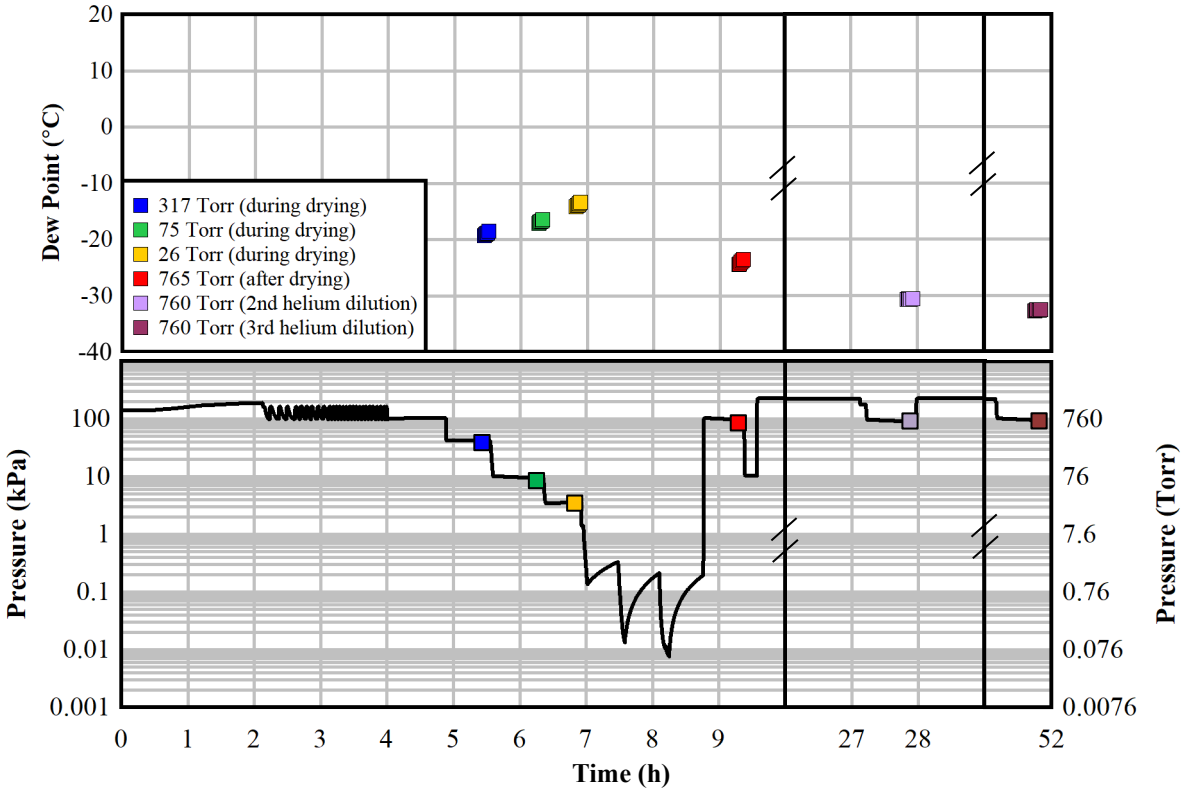

Figure 3-11 Dew points (top) and pressure (bottom) histories during simulated drying of the DDA with an open guide tube and deionized water on 02/08/22.

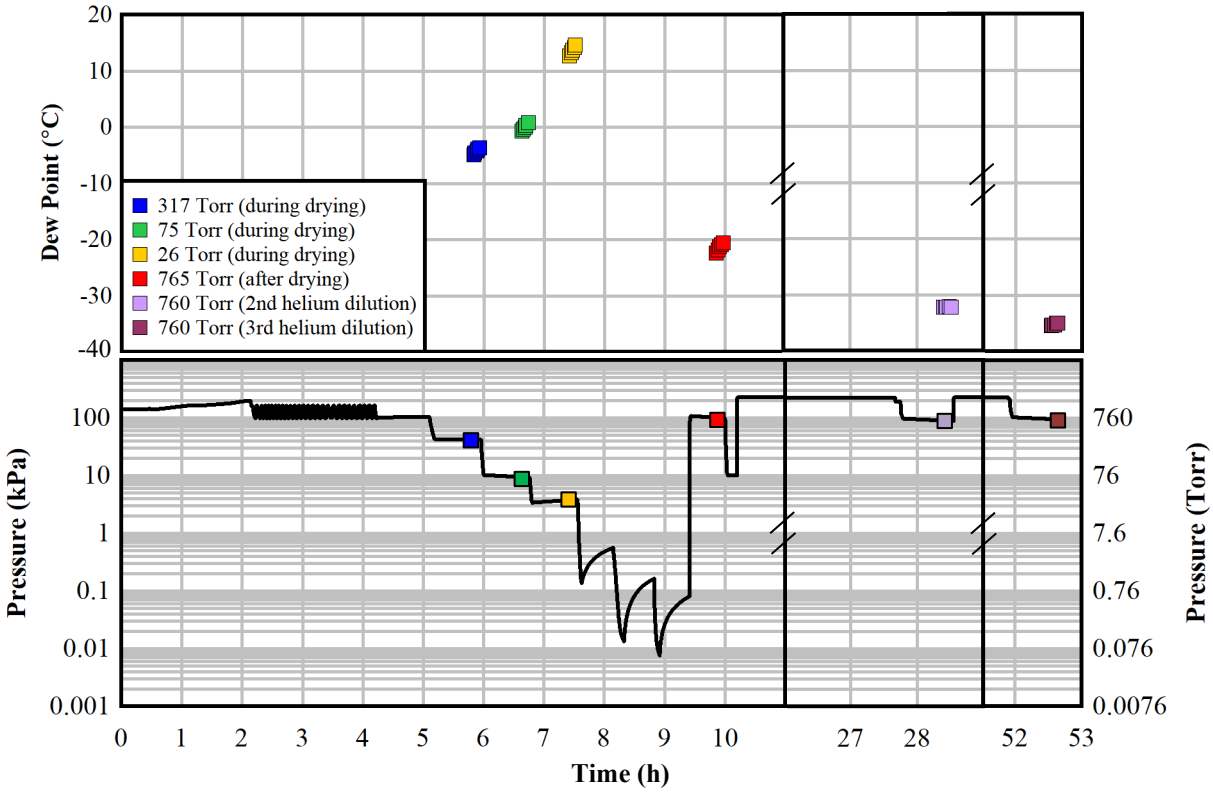

Figure 3-12 Dew points (top) and pressure (bottom) histories during simulated drying of the DDA with an open guide tube and 0.2 M boric acid on 02/16/22.

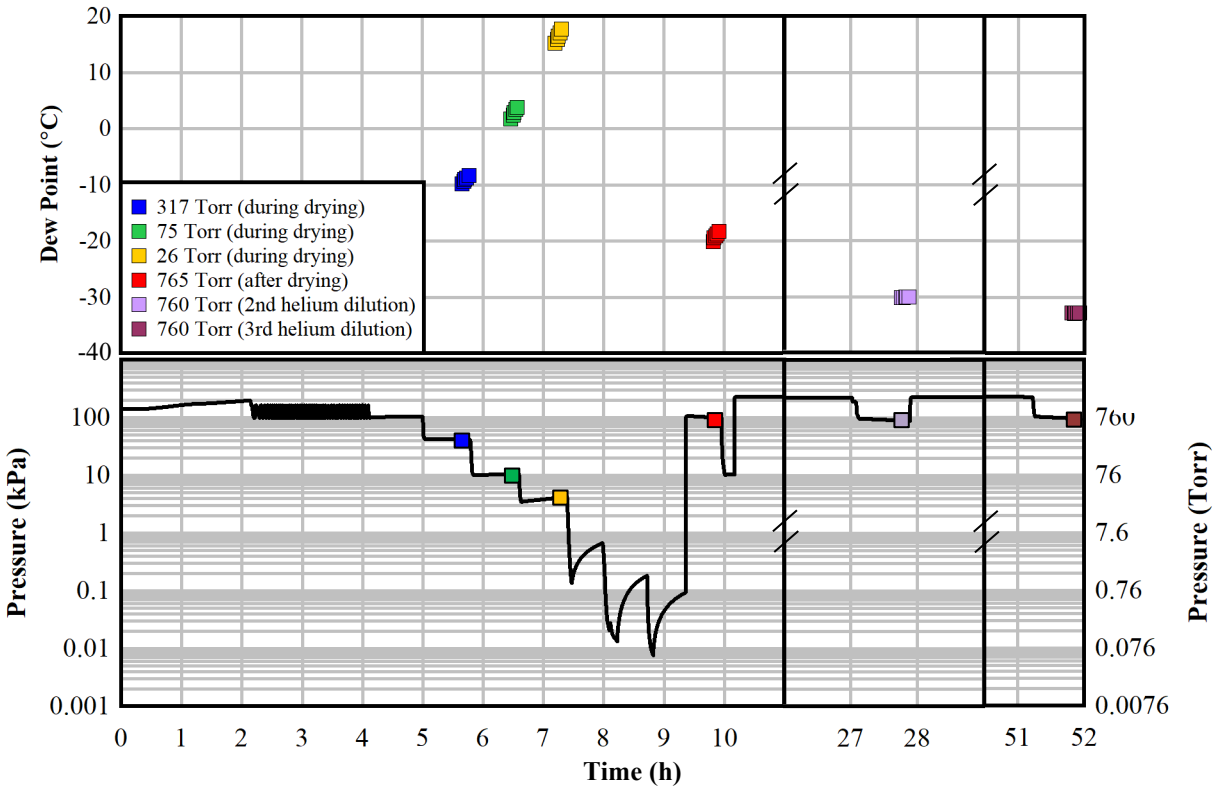

Figure 3-13 Dew points (top) and pressure (bottom) histories during simulated drying of the DDA with an open guide tube and 0.2 M boric acid on 03/02/22.

Although at least 30 measurements are taken during the various vacuum isolations, each measurement takes about 60-90 seconds to complete, and it takes about 15 measurements for the MS water content to approach a steady value. A 45-minute sample period was chosen to accommodate for both the MS vacuum reducing the pressure of the sample and keeping the time scale factor between HBDP drying and DDA testing as close to two as possible. The reported values are the averages of five measurements following steady state. Also shown in Table 3-3 is the calculated dew point of the gas at both the sampling and hold pressures. The predicted water content based on the dilution factor (the dilution factor being the ratio between the high pressure hold and DDA sampling pressures) is the expected water content value that would be measured if the water vapor was uniformly distributed in the DDA backfill gas. It would be expected that the helium backfill would result in reduced water content – the quantity of water remains the same and the quantity of helium increases during helium backfill, and the ratio of water to helium remains the same as vacuum is applied and the backfill gas is evacuated from the DDA. The inconsistencies between the predicted and the measured water content with each helium dilution suggests that the water vapor being evacuated from the DDA cannot be entirely accounted for by the introduction of additional helium and the subsequent reduction in water content. The differences between the predicted and measured water content values merits further investigation into the mechanisms behind water adsorption that could potentially explain these inconsistencies.

The similarity in water content values between the 02/16/22 and the 03/02/22 tests serve to demonstrate repeatability given the same input parameters, which attests to excellent control over the system variables despite the large swings in pressure and vacuum levels as well as added assurance in the accuracy of the data presented in this report.

The water content measurements following the drying procedure for all tests did not exceed 1,200 ppm_v. These values are about one order of magnitude lower than the 10,000 and 17,400 ppm_v water content

measurements made for the HBDP cask (Bryan *et al.*, 2019). The differences could be attributed to a number of factors. One factor could be the previously acknowledged scaling distortions between the HBDP cask that contains multiple assemblies, a basket, and neutron poisons. In comparison the DDA houses a cutout of a single assembly and a single dashpot region and therefore has a reduced number of water retention sites compared to the HBDP cask (40:1 cask internals to cask wall surface area ratio for the HBDP compared to a 2.5:1 vessel internals to vessel wall surface area ratio for the DDA). Another factor could be water sorption in the sampling lines, which was an issue acknowledged in the HBDP gas sampling study. This issue was explicitly addressed in the DDA setup through the addition of heat trace cabling on the sample lines, which prevented moisture build-up and maximized the likelihood of the source of measured water content as originating from the DDA fill fluid.

3.5 Boric Acid Characterization for Post-Drain Blowdown Fluid

Post-drain/blowdown solution samples were tested for pH, density, and boron, iron, and nickel concentration, shown in Table 3-4. These samples were diluted to both 1:10 and 1:100 samples. Standards were made to test within a range of 50 ppm_m and 0.5 ppm_m. The ICP OES tested each sample three times and reported the average. The 1:10 samples were meant to capture boron in the washes as well as any potential iron or nickel to ensure the acid had not corroded the inside of the vessel. Again, results from the ICP OES were multiplied by 10 or 100 as appropriate and then reported in Table 3-4.

As previously stated, the measurement accuracy is reported by the correlation coefficient (R). The closer to the value is to 1, the better the standard and the more accurate the results. For boron, R = 0.999674 for the February samples and R = 0.999853 for the March samples. For iron and nickel, R = 0.999967 and R = 0.999969, respectively, for the February samples; R = 0.999897 and R = 0.999700, respectively, for the March samples. The RSD values for boron are also reported in the table. The R values were all close to 1, but those values could be improved. The RSD values for iron and nickel are not reported as iron and nickel were below the detection limit in all samples.

The boron concentration was higher than the concentration seen in Table 2-3 in both post-drain/blowdown samples. This is likely due to measurement precision, which is quantified by the RSD. The post-drain/blowdown pH values were slightly less acidic, which is due to some conjugate acid, H_3O^+ (shown in Equation 2-2) being left in the system. This is shown further from the pH of the washes, seen in Table 3-4. Some of the boron was also left in the canister after drying, as shown by the boron concentrations of 55 ppm_m for the 02/21 wash and 56 ppm_m for the 03/07 wash. The sample from the second wash done for the 03/02/22 test showed the pH decreasing by 0.15 compared to the first wash sample. It is not immediately known what caused this, but it could be due to the inhomogeneity of the solution leading to a non-representative sample or errors in the pH meter. The boron concentration after the second wash decreased to 22 ppm_m, which was expected. It is important to note that more water was used to wash the canister than was used for the tests. This was to ensure a thorough wash, but by using Equation 3-1, the amount of H_3O^+ is calculated and shown for each wash in Table 3-5. Both washes had lower concentrations than the pre-test and post-test samples by at least a factor of 10. The concentration did increase from wash 1 to wash 2, which tracks with the lower, more acidic pH in wash 2, mentioned above. Nickel and iron were below the detection limit in every sample, showing that no corrosion occurred over the course of the experiment, which was expected.

Table 3-4 ICP OES analysis of post-DDA test samples.

Sample ID	pH	Density	Boron Concentration (ppm_m)	Boron RSD (%)	Iron Concentration (ppm_m)	Nickel Concentration (ppm_m)
02/16 Post DDA	4.82	1.00	2780	0.53	< 5	< 5
02/21 Wash	5.87	0.99	55	0.34	< 5	< 5
03/02 Post DDA	4.87	1.00	2750	0.98	< 5	< 5
03/07 Wash 1	5.85	0.99	56	0.90	< 5	< 5
03/07 Wash 2	5.70	1.00	22	0.17	< 5	< 5

$$H_3O^+(mol) = \frac{10^{-pH}(W)}{2.2}$$ Equation 3-1

Table 3-5 Measured pH and moles of acid of pre- and post-DDA test samples.

Sample	pH	H_3O^+ (mol)
02/15 Pre DDA	4.73	8.55E-05
02/16 Post DDA	4.82	6.95E-05
02/21 Wash	5.87	6.44E-06
03/01 Pre DDA	4.79	7.45E-05
03/02 Post DDA	4.87	6.19E-05
03/07 Wash 1	5.85	6.87E-06
03/07 Wash 2	5.70	9.70E-06

4 SUMMARY

Validation of the extent of water removal in a dry spent nuclear fuel storage system based on drying procedures used at nuclear power plants is needed to close existing technical gaps. Operational conditions leading to incomplete drying may have potential impacts on the fuel, cladding, and other components in the system. A general lack of data suitable for model validation of commercial nuclear canister drying processes necessitates additional, well-designed investigations of drying process efficacy and water retention. Scaled tests that incorporate relevant physics and well-controlled boundary conditions are essential to provide guidance to the simulation of prototypic systems undergoing drying processes. The use of boric acid solutions in these scaled tests allows for more accurate representation of spent fuel pool conditions.

4.1 Dashpot Drying Apparatus

A new small-scale pressure vessel with a 5×5 fuel assembly and axially-truncated PWR hardware was created to simulate commercial vacuum drying processes. This test assembly, known as the Dashpot Drying Apparatus (DDA), was built to focus on the drying of a single PWR dashpot and surrounding fuel. Drying operations were simulated for three tests with the DDA based on the pressure and temperature histories observed in the High Burnup Demonstration Project (HBDP). All three tests were conducted with an empty guide tube. One test was performed with deionized water as the fill fluid. The other two tests used 0.2 M boric acid as the fill fluid to accurately simulate spent fuel pool conditions. These tests proved the capability of the DDA to mimic commercial drying processes on a limited scale and detect the presence of bulk and residual water. Furthermore, for all tests, pressure remained below the 0.4 kPa (3 Torr) rebound threshold for the final evacuation step in the drying procedure.

The instrumentation, power control, and MS of the DDA functioned as designed. However, limitations on the maximum temperature of the external flexible heaters somewhat limited peak cladding temperatures compared to the HBDP. An improvement to previous DDA testing (Durbin *et al.*, 2021) included uniform power supply to the external heaters across all three tests presented in this report as well as adding heat trace cabling and insulation along the pressure and vacuum lines to prevent condensation and subsequent skewing of MS water content measurements. Another improvement involved measurement of the water content in the DDA following a drying and heating step, which was conducted before every test. Measurements of water content below 100 ppm_v following system drying ensured that any water content detected by the MS was from the fill fluid.

Table 4-1 summarizes the mass spectrometer water content from the DDA tests. The results show that despite high initial water content measured during the drying procedure, after the vacuum isolations the water content in all tests drops to below 1,200 ppm_v, demonstrating that the drying procedure effectively removed water from the DDA vessel. Scaling distortions between the HBDP cask and the DDA exist due to the inclusion of additional assemblies, dashpot regions, the basket surrounding the assemblies, and the neutron poisons in the HBDP that are absent from the DDA. Regardless, the DDA results can be interpreted as the quantification of water retention potential from a single dashpot region using well-controlled boundary conditions.

Table 4-1 Mass spectrometer water content data summary for the DDA tests.

Sampling Date	Fill Fluid	Test Step	High Pressure Hold, P_{Hold} (kPa)	Vessel Sampling Pressure P_{Sample} (kPa)	Measured Water Content (ppm_v)
2/8/2022	DI Water	1st vacuum isolation	--	42.3	2,761
2/8/2022		2nd vacuum isolation	--	10.0	15,304
2/8/2022		3rd vacuum isolation	--	3.47	53,087
2/8/2022		1st helium backfill	102	102	739
2/9/2022		2nd helium backfill	222	100	402
2/10/2022		3rd helium backfill	222	100	306
2/16/2022	0.2 M Boric Acid	1st vacuum isolation	--	42.3	10,383
2/16/2022		2nd vacuum isolation	--	10.0	66,973
2/16/2022		3rd vacuum isolation	--	3.47	422,200
2/16/2022		1st helium backfill	102	102	920
2/17/2022		2nd helium backfill	222	100	345
2/18/2022		3rd helium backfill	222	100	234
3/2/2022	0.2 M Boric Acid	1st vacuum isolation	--	42.3	6,916
3/2/2022		2nd vacuum isolation	--	10.0	72,978
3/2/2022		3rd vacuum isolation	--	3.47	462,357
3/2/2022		1st helium backfill	102	102	1,155
3/3/2022		2nd helium backfill	222	100	432
3/4/2022		3rd helium backfill	222	100	303

The ICP OES analysis showed that most boron was recovered from the drying process. Only about 50 ppm_m, or roughly 0.2 grams, of boron was recovered after washing the DDA with DI water, and 25 ppm_m, roughly 0.1 gram, was recovered after a second wash. Most of the acid was also removed in the drying process, but about 1.5×10^{-4} grams of acid were recovered after the first wash and 6.6×10^{-5} grams of acid were recovered after the second wash. This was also seen by the increasingly higher pH of the samples after each wash. No iron or nickel was found in the samples, showing that no immediate corrosion of the material occurred during the test, which was the expected outcome as the canister is made of stainless steel.

4.2 Future Work

The data and operational experience gained from the DDA test series is expected to guide and improve the next drying test, which is based on a partially-submersible, full-scale PWR fuel assembly.

Termed the Advanced Drying Cycle Simulator (ADCS), this next drying test series is currently planned to bridge the prototypic complexity of the HBDP and the focused scale of the DDA. This new apparatus will use a prototypic 17×17 commercial PWR skeleton populated with submersible electrically resistive heaters and will feature a specialized test rod. The fuel length would be prototypic and generate realistic temperature gradients, all while maintaining the intricate features of the guide tubes and grid spacers.

A pressure vessel concept for housing the specialized assembly is shown in Figure 4-1. The PV is comprised of two sections of nominal 14 in. pipes joined by welded flanges with ring-type joints, where the smaller pipe at the bottom is designed specifically to accommodate thermocouple compression fittings. Water would fill and drain through the welded siphon tube welded to the upper portion of the top

pipe. This is meant to better represent a commercial canister system, where no lower drain is possible. The mass spectrometer would have a direct sampling port near the top of the pressure vessel and would be placed near other penetrations for electrical power feeds and pressure.

A removable test rod can be used for internal pressure monitoring or representations of breached rods. Heaters would comprise the majority of rod positions in the skeleton and be of uniform electrical resistance. The test rod would be located at the very center of the assembly and serve as a flexible and replaceable testing component fed through an opening in the pressure vessel.

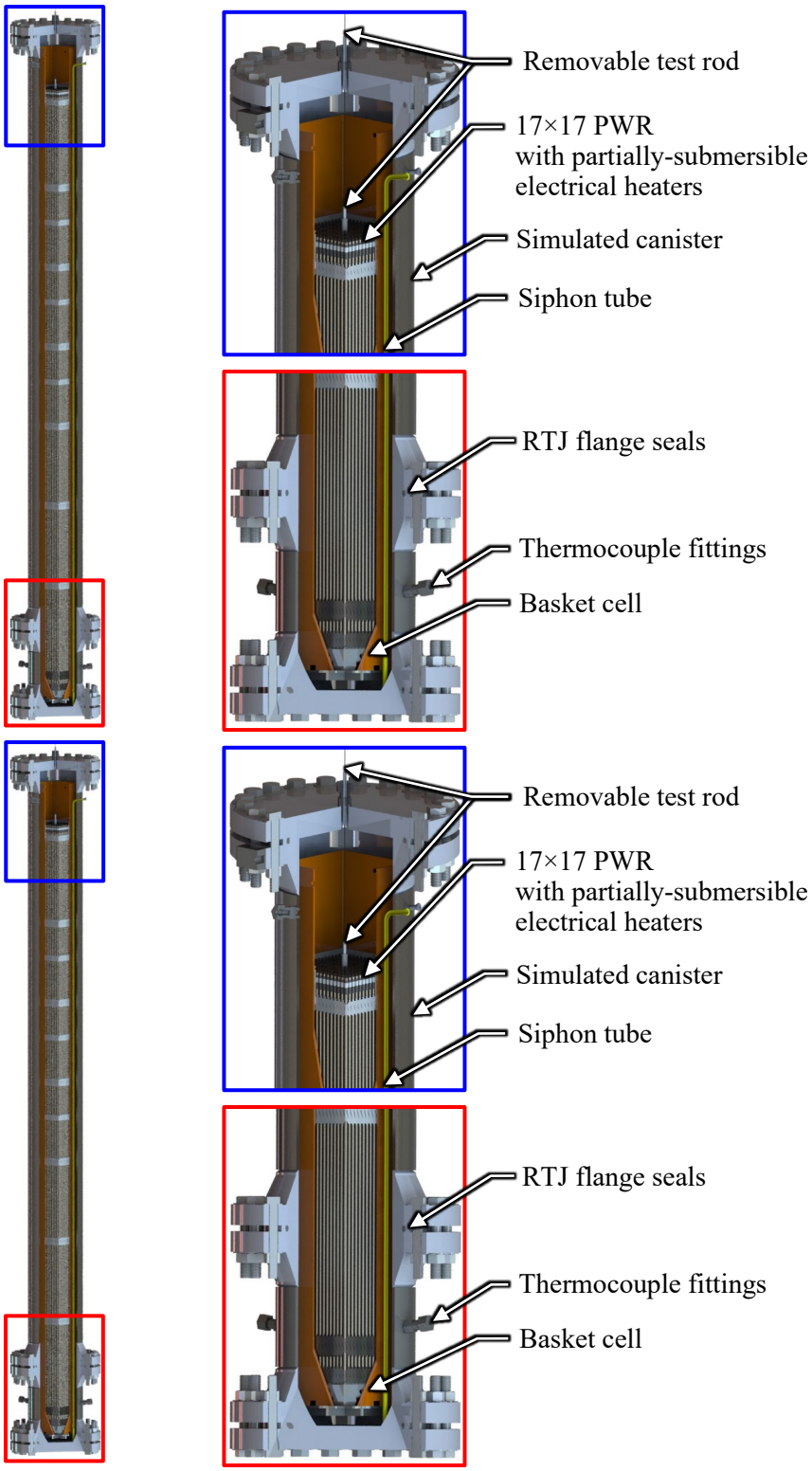

Figure 4-1 Schematic of the Advanced Drying Cycle Simulator using a prototypic-length 17×17 PWR test assembly.

5 REFERENCES

ASTM International (2016). Standard Guide for Drying Behavior of Spent Nuclear Fuel (C1553-16). ASTM Book of Standards Volume 12.01. West Conshohocken, PA.

ASTM International (2017). Standard Specification for Temperature-Electromotive Force (emf) Tables for Standardized Thermocouples (E230/E230M-17). ASTM Book of Standards Volume 14.03. West Conshohocken, PA.

Bryan, C. R., Jarek, R. L., Flores, C., & Leonard, E. (2019). Analysis of Gas Samples Taken from the High Burnup Demonstration Cask (SAND2019-2281). Sandia National Laboratories. Albuquerque, NM.

Comanche Peak Steam Electric Station. (2000). Spent Fuel Pool Boron Dilution Analysis (ER-ME-105 Rev. 2). Comanche Peak Steam Electric Station. Glen Rose, TX.

Combustion Engineering Inc. (1986). Boric Acid Makeup Tank Concentration Reduction Effort Technical Bases and Operational Analysis. (CEN-316(S)). Combustion Engineering Inc. Windsor, CT.

Colburn, H. A. (2021). Small Scale Drying: FY21 Interim Report. PNNL-31749. Pacific Northwest national Laboratory, Richland, WA.

EPRI. High Burnup Dry Storage Research Project Cask Loading and Initial Results (2019). Technical Report 3002015076. Palo Alto, CA.

Durbin, S.G., E.R. Lindgren, R.J.M. Pulido, A. Salazar III, and R.E. Fasano (2021). Update on the Simulation of Commercial Drying of Spent Nuclear Fuel (SAND2021-11828 R). Sandia National Laboratories. Albuquerque, NM.

Fort, J. A., Richmond, D. J., Jensen, B. J., & Suffield, S. R. (2019). High-Burnup Demonstration: Thermal Modeling of TN-32B Vacuum Drying and ISFSI Transients (PNNL-29058). Pacific Northwest National Laboratories. Richland, WA.

Hanson, B. D., & Alsaed, H. A. (2019). Gap Analysis to Support Extended Storage and Transportation of Spent Nuclear Fuel: Five-Year Delta (SFWD-SFWST-2017-000005, Rev 1; PNNL-28711). Pacific Northwest National Laboratory. Richland, WA.

Harden, P. A. (2001). Palisades Nuclear Plant Supplemental Information to Technical Specification Change Request – Spent Fuel Pool Boron Concentration. (Docket 50-255 – License DPR-20). Palisades Nuclear Plant. Covert, MI.

Hiden Analytical Limited (2018). TWN QIC Dual Stage Sampling Head manual (HA-085-850). Warrington, United Kingdom.

IAEA. (1982). Storage of Water Reactor Spent Fuel in Water Pools: Survey of World Experience. (Technical Report Series No. 218). International Atomic Energy Agency. Vienna, Austria.

Johnson Jr., A. B. (1977). Behavior of Spent Nuclear Fuel in Water Pool Storage. (BNWL-2256; UC-70). Battelle Pacific Northwest Laboratories. Richland, WA.

Knight, T. W. (2019). Experimental Determination and Modeling of Used Fuel Drying by Vacuum and Gas Circulation for Dry Cask Storage (NEUP 14-7730). University of South Carolina. Columbia, SC.

Knoll, R., & Gilbert, E. (1987). Evaluation of Cover Gas Impurities and their Effects on the Dry Storage of LWR (Light-Water Reactor) Spent Fuel (PNL-6365). Pacific Northwest National Laboratory. Richland, WA.

Nuclear Regulatory Commission (2002). Westinghouse Technology Manual (ML023040131). Washington, D.C.

Nuclear Regulatory Commission (2002). TN-32 Final Safety Analysis Report (FSAR), Revision 2. Washington, D.C.

Nuclear Regulatory Commission (2010). Standard Review Plan for Spent Fuel Dry Storage Systems at a General License Facility (NUREG-1536). Washington, D.C.

Nuclear Regulatory Commission (2011). Corrosion and Corrosion Control in LWRs. Washington, D.C.

Salazar, A., Pulido, R. JSF. M., Lindgren, E. R., & Durbin, S. G. (2019). Advanced Concepts for Dry Storage Cask Thermal-Hydraulic Testing (SAND2019-11281 R). Sandia National Laboratories. Albuquerque, NM.

Salazar, A., Lindgren, E. R., Fasano, R. E., Pulido, R. J. M., & Durbin, S. G. (2020). Development of Mockups and Instrumentation for Spent Fuel Drying Tests (SAND2020-5341 R). Sandia National Laboratories, Albuquerque, NM.

APPENDIX A LIST OF INTERNAL, EXTERNAL, AND AMBIENT THERMOCOUPLES IN DDA TEST SETUP

Table A-1 List of internal thermocouples in DDA test setup.

#	Type	Coordinate	*z* Position (in.)	Direction (Degrees)	DAQ Label
1	T	GT_D2	0.00	45°	GT_D2_0.00"
2	T	GT_D2	0.875	45°	GT_D2_0.875"
3	T	GT_D2	1.625	45°	GT_D2_1.625"
4	T	GT_D2	2.50	45°	GT_D2_2.50"
5	T	GT_D2	4.25	45°	GT_D2_4.25"
6	T	GT_D2	9.625	45°	GT_D2_9.625"
7	T	GT_D2	15.00	45°	GT_D2_15.00"
8	T	GT_D2	20.375	45°	GT_D2_20.375"
9	T	GT_D2	25.6875	45°	GT_D2_25.6875"
10	T	A1	2.50	315°	A1_2.50"
11	T	A1	9.625	315°	A1_9.625"
12	T	A1	20.375	315°	A1_20.375"
13	T	A3	2.50	225°	A3_2.50"
14	T	A3	9.625	225°	A3_9.625"
15	T	A3	20.375	225°	A3_20.375"
16	T	A5	0.00	45°	A5_0.00"
17	T	A5	15.00	45°	A5_15.00"
18	T	A5	25.6875	45°	A5_25.6875"
19	T	C3	0.00	135°	C3_0.00"
20	T	C3	2.50	135°	C3_2.50"
21	T	C3	4.25	135°	C3_4.25"
22	T	C3	9.625	135°	C3_9.625"
23	T	C3	15.00	135°	C3_15.00"
24	T	C3	20.375	135°	C3_20.375"
25	T	C3	25.6875	135°	C3_25.6875"
26	T	E1	0.00	225°	E1_0.00"
27	T	E1	15.00	225°	E1_15.00"
28	T	E1	25.6875	225°	E1_25.6875"
29	T	E3	0.00	315°	E3_0.00"
30	T	E3	2.50	315°	E3_2.50"
31	T	E3	4.25	315°	E3_4.25"
32	T	E3	15.00	315°	E3_15.00"
33	T	E3	25.6875	315°	E3_25.6875"
34	T	E5	0.00	135°	E5_0.00"
35	T	E5	2.50	135°	E5_2.50"
36	T	E5	4.25	135°	E5_4.25"

#	Type	Coordinate	*z* Position (in.)	Direction (Degrees)	DAQ Label
37	T	E5	15.00	135°	E5_15.00"
38	T	E5	25.6875	135°	E5_25.6875"
39	T	PV	-2.50	-	PV_Interior_BottomFlange
40	T	PV	2.50	-	PV_Interior_2.50"

Table A-2 List of external (Ext.) and ambient (Amb.) thermocouples in DDA test setup.

#	Type	Surface	Location	*z* Position (in.)	Direction (Degrees)	DAQ Label
41	T	Ext.	PV	0.00	0°	PV_0°_0.00"
42	T	Ext.	PV	0.88	0°	PV_0°_.875"
43	T	Ext.	PV	1.63	0°	PV_0°_1.625"
44	T	Ext.	PV	2.50	0°	PV_0°_2.50"
45	T	Ext.	PV	4.25	0°	PV_0°_4.25"
46	T	Ext.	PV	9.63	0°	PV_0°_9.625"
47	T	Ext.	PV	15.00	0°	PV_0°_15.00"
48	T	Ext.	PV	20.38	0°	PV_0°_20.375"
49	T	Ext.	PV	25.69	0°	PV_0°_25.6875"
50	T	Ext.	PV	15.00	90°	PV_90°_15.00"
51	T	Ext.	PV	2.50	135°	PV_135°_2.50"
52	T	Ext.	PV	25.69	180°	PV_180°_25.6875”
53	T	Ext.	PV	34.08	-	PV_TopFlange
54	T	Ext.	PV	-4.33	-	PV_BottomFlange
61	T	Amb.	Mount	-5.00	-	Ambient_1_-5”
62	T	Amb.	Mount	14.50	-	Ambient_2_14.5”
63	T	Amb.	Mount	32.25	-	Ambient_3_35.25”

Sandia National Laboratories